Kinetics and Mechanism of the Insertion of Olefins into Niobium- and Tantalum-Hydride Bonds: A Study of the Competition between Steric and Electronic Effects

Barbara J. Burger, Bernard D. Santarsiero, Mark S. Trimmer, and John E. Bercaw*

Contribution No. 7594 from the Division of Chemistry and Chemical Engineering, California Institute of Technology, Pasadena, California 91125. *Received May 18, 1987*

Abstract: The mechanism of insertion of olefins into transition metal–hydride bonds has been examined for a series of olefin hydride complexes of niobocene, permethylniobocene, tantalocene, and permethyltantalocene. The insertion rates were measured for several meta-substituted styrene complexes of permethylniobocene and found to be comparable to those found for the para-substituted analogues, indicating that the electronic effects are largely inductive in origin. An X-ray crystal structure determination for the parent styrene complex (P_{bca}; a = 14.626 (3) Å, b = 18.134 (4) Å, c = 18.147 (4) Å; α, β, γ = 90°) offers an explanation for this observation: the phenyl ring is bent out of resonance with the olefin π system by 32°. A comparison of the rates for the entire series of ethylene compounds (where steric effects are minimal) indicates that there are significant electronic effects acting within this family ($k_{Nb} > k_{Ta}$ and $k_{Cp} > k_{Cp^*}$; Cp = (η^5-C_5H_5), Cp* = (η^5-C_5Me_5)). In contrast to the pentamethylcyclopentadienyl systems for which steric interactions appear to dominate, the normal cyclopentadienyl compounds are virtually insensitive to sterics, allowing for the existence of two isomeric forms of the α-olefin hydride complexes (endo, olefin substituent central, and exo, olefin substituent lateral in the equatorial plane) in roughly 1:1 proportion. The series of propylene hydride compounds, while showing some electronic effects ($k_{Nb} > k_{Ta}$), further demonstrates the importance of steric interactions in determining the rates of olefin insertion ($k_{Cp^*} > k_{Cp}$). A thermodynamic and kinetic analysis has been completed for a series of niobocene styrene hydride complexes to better define the electronic requirements for the [(η^5-C_5H_5)$_2$Nb] derivatives, a system where the interfering steric interactions are minimized. The ground-state orderings ($\Delta G°$) are strongly dependent upon the para substituent (ρ = +2.2). The insertion rates for the endo and exo forms are also dependent on the substitution of the phenyl ring, and ρ values of −1.1 and +0.7, respectively, have been measured. These results are interpreted in terms of a concerted four-center model with moderate positive charge buildup at the β-carbon and, in the case of the endo isomer, competing ground- and transition-state effects.

Olefin insertion into metal–hydrogen bonds and its microscopic reverse, β-H elimination, are very common in organometallic chemistry, yet few mechanistic studies of these fundamental transformations have been carried out.[1,2] Previous investigations in our research group have focused on the first of these transformations, olefin insertion into Nb–H bonds, and we have examined a series of olefin hydride complexes of permethylniobocene, Cp*$_2$Nb(CH$_2$=CHR)H (Cp* = η^5-C_5Me_5; R = H, Me, Ph, C_6H_4-p-X (X = CF_3, Me, OMe, NMe_2))[2] Even where R ≠ H, a single isomer is formed, which from NMR data[2b] and steric considerations was shown to be that with the olefin substituent R located at the endo (central, less crowded) position of the equatorial plane of the bent sandwich structure.

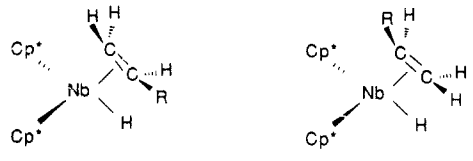

endo *exo*

Insertion of olefin into the Nb–H bond (k_1) is reversible, and a lower limit for k_{-1} (>100k_1) can be estimated (eq 1) from the undetectably small concentrations (^{1}H NMR) of the alkyl tautomer. Interception of the coordinatively unsaturated intermediate

$$Cp^*_2Nb(CH_2{=}CHR)H \underset{k_{-1}}{\overset{k_1}{\rightleftharpoons}} [Cp^*_2Nb{-}CH_2CH_2R] \xrightarrow[L]{k_2} Cp^*_2Nb(CH_2CH_2R)L \quad (1)$$

by an external ligand (L = CO, $CNCH_3$) is much slower than β-H elimination, so that the rate of formation of Cp*$_2$Nb(CH$_2$CH$_2$R)L follows second-order kinetics, first order in both [Cp*$_2$Nb(CH$_2$=CHR)H] and [L], even at the highest practical concentrations of trapping ligand, L. Thus, values for the k_1's in eq 1 were not directly obtainable from kinetics of these ligand-trapping experiments.

The rates of insertion of olefins into the Nb–H bond (k_1) were, however, determined by magnetization transfer and coalescence techniques (^{1}H NMR), and a model for the insertion process for the permethylniobocene system has been developed: olefin insertion proceeds via a four-center transition state with partial positive charge development at the β-carbon of the incipient metal alkyl.[3]

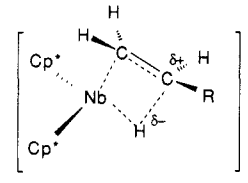

Electronic effects on the ground states of Cp*$_2$Nb(CH$_2$=CHC$_6$H$_4$-p-X)H were found to be small, but a modest effect on the relative transition-state energies is evident from the differing rates of olefin insertion for various para-substituted styrenes. Electronic effects can be transmitted either through the σ framework (induction) or the styrene π system (resonance). An approximate measure of the relative contributions of these two different modes of transmission can be gained through a comparative study of the rates of insertion for meta- and para-sub-

(1) (a) Halpern, J.; Okamoto, T.; Zakchariev, A. *J. Mol. Catal.* **1976**, *2*, 65–68. (b) Byrne, J. W.; Blaser, H. U.; Osborn, J. A. *J. Am. Chem. Soc.* **1975**, *97*, 3871–3873. (c) Chaudret, B. N.; Cole-Hamilton, D. J.; Wilkinson, G. *Acta Chem. Scand., Ser. A* **1978**, *A32*, 763–769. (d) Pardy, R. A.; Taylor, M. J.; Constable, E. C.; Mersh, J. D.; Sanders, J. K. M. *J. Organomet. Chem.* **1981**, *231*, C25–C30. (e) Roe, D. C. *Abstracts of Papers*, XIth International Conference on Organometallic Chemistry, Callaway Gardens, Pine Mountain, Georgia, Oct 10–14, 1983; p 133. (f) Roe, D. C. *J. Am. Chem. Soc.* **1983**, *105*, 7771–7772. (g) Halpern, J.; Okamoto, T. *Inorg. Chim. Acta* **1984**, *89*, L53–L54.

(2) (a) McGrady, N. D.; McDade, C.; Bercaw, J. E. In *Organometallic Compounds: Synthesis, Structure, and Theory*; Shapiro, B. L., Ed.; Texas A&M University Press: College Station, TX, 1983; pp 46–85. (b) Doherty, N. M.; Bercaw, J. E. *J. Am. Chem. Soc.* **1985**, *107*, 2670–2682.

(3) C_α and C_β designations of substituent locations will be in reference to the metal alkyl rather than the free olefin.

0002-7863/88/1510-3134$01.50/0 © 1988 American Chemical Society

stituted styrenes. Meta-substituent effects on the reaction rate are transmitted principally through induction, whereas combined resonant and inductive effects operate for the para-substituted styrenes.[4] Hence, a series of meta-substituted styrene hydride complexes of permethylniobocene has been prepared, and the rates of olefin insertion for these complexes were measured by coalescence techniques (^{1}H NMR) for comparison to the analogous para-substituted styrene hydrides.[2] In addition, a crystal structure determination of the parent styrene hydride complex, $Cp^*_2Nb(CH_2{=}CHC_6H_5)H$ (**2**), was carried out in order to test the validity of our assumption that the phenyl ring is twisted out-of-resonance, thus attenuating the substituent effects on the ground state.[2b]

In view of the relatively large steric effects established for the permethylniobocene system by these and earlier studies, it was of interest to undertake a complementary study of the olefin insertion process in a system where steric considerations would be greatly diminished. Electronic effects are more easily probed when interfering steric effects are minimized. Moreover, the substitution of (η^5-C_5H_5) for the bulkier (η^5-C_5Me_5) rings also permitted the ancillary ligand electronic effects to be examined. For example, to the extent that the olefin hydride complex is formally Nb^V (considering the metal–olefin bonding in the niobacyclopropane limit) and the insertion product is formally Nb^{III}, the more electron-releasing (η^5-C_5Me_5) ligands would be expected to exhibit slower rates of olefin insertion due to stabilization of the ground state relative to the transition state, the latter more closely resembling the insertion product according to the Hammond postulate.[5] Interestingly, the steric and electronic effects of methyl substitution of the two cyclopentadienyl rings are predicted to operate in opposite directions, since sterically demanding pentamethylcyclopentadienyl ligands should destabilize the more crowded ground state relative to the transition state. Thus, such a comparative study of $[Cp_2Nb]$ versus $[Cp^*_2Nb]$ should allow the relative importance of electronic and steric effects to be determined. Accordingly, a series of olefin hydride complexes of bis(cyclopentadienyl)niobium, $Cp_2Nb(CH_2{=}CHR)H$ (Cp = (η^5-C_5H_5); R = H, CH_3, C_6H_5, C_6H_4-*p*-X (X = CF_3, OMe, NMe_2)), has been prepared. Some of these niobocene olefin hydride derivatives have been previously described[6] and exist as nearly equal proportions of the endo and exo isomers, presumably due to reduced steric demands in these systems. The relative ground-state energies and rates of olefin insertion for these complexes have been measured for comparison to the permethylniobocene system. Since we have recently developed a synthetic entry into olefin hydride derivatives of permethyltantalocene,[7] we have also undertaken measurement of olefin insertion rates for these complexes and their tantalocene analogues synthesized previously[6b,d] to provide quantitative differences in rates between analogous compounds for members of the second and third row of the group 5 triad.

Herein we report the results of studies of the kinetics for olefin insertion for $Cp^*_2Nb(CH_2{=}CHC_6H_4$-*m*-X)H (X = CF_3, CH_3, NMe_2), $Cp_2Nb(CH_2{=}CHC_6H_4$-*p*-X)H (X = CF_3, H, OMe, NMe_2), and $Cp_2Nb(CH_2{=}CHR)H$, $Cp^*_2Ta(CH_2{=}CHR)H$, and $Cp_2Ta(CH_2{=}CHR)H$ (R = H, CH_3) together with the results of a crystal structure determination for $Cp^*_2Nb(CH_2{=}CHC_6H_5)H$.

Results

Synthesis and Characterization of Meta-Substituted Styrene Hydride Complexes of Permethylniobocene. Treatment of $Cp^*_2NbH_3$ (**1**) with an excess (5 to 6 equiv) of the appropriate meta-substituted styrene in toluene at 80 °C for 1 day affords the styrene hydride complexes **3–5**. One equivalent of the corresponding phenylethane, *m*-X-$C_6H_4CH_2CH_3$, is formed concomitantly. The desired compounds are isolated by extraction and crystallization from petroleum ether. The yields vary with styrene but typically range from 50 to 80%.

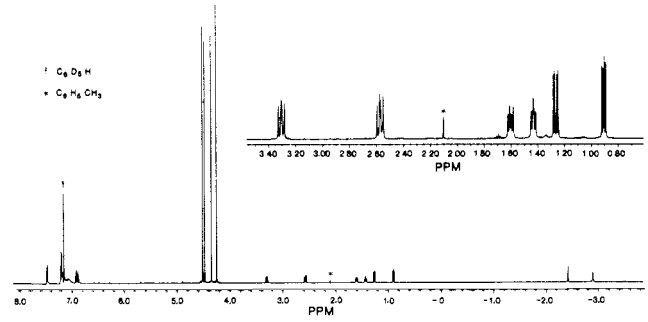

Figure 1. 500-MHz ^{1}H NMR spectrum of *exo*- and *endo*-$Cp_2Nb(H_2C{=}CHC_6H_5)H$ (nonequilibrium mixture of isomers).

$$Cp^*_2NbH_3 + 2\,m\text{-X-}C_6H_4CH{=}CH_2 \xrightarrow[80\ °C]{\text{toluene}} Cp^*_2Nb(CH_2{=}CHC_6H_4\text{-}m\text{-X})H + m\text{-X-}C_6H_4CH_2CH_3 \quad (2)$$

3: X = CF_3
4: X = CH_3
5: X = NMe_2

The ^{1}H NMR spectra of the meta styrene hydride complexes (see Table I) are all similar and are analogous to those obtained for the para styrene hydride complexes.[2b] The ^{13}C–H coupling constants, measured in the gated (^{1}H NOE enhanced) ^{13}C NMR spectra for **3–5**, are in the range 140–146 Hz (see Table I) and are indicative of substantial metallacyclopropane character (Nb^V) vis-à-vis a formal Nb^{III}–olefin adduct, similar to other complexes of d^2 bent metallocenes.[2b,6,8]

Synthesis and Characterization of Para-Substituted Styrene Hydride Complexes of Niobocene. In an analogous fashion to that described above, the niobocene styrene hydride compounds $Cp_2Nb(CH_2{=}CHC_6H_4$-*p*-X)H (**7–10**) are conveniently prepared by treatment of Cp_2NbH_3 (**6**) with the appropriate styrene.

$$Cp_2NbH_3 + 2\,p\text{-X-}C_6H_4CH{=}CH_2 \xrightarrow[25\ °C]{\text{toluene}} Cp_2Nb(CH_2{=}CHC_6H_4\text{-}p\text{-X})H + p\text{-X-}C_6H_4CH_2CH_3 \quad (3)$$

7: X = H
8: X = CF_3
9: X = OMe
10: X = NMe_2

As before, 1 equiv of the hydrogenated olefin, *p*-X-$C_6H_4CH_2CH_3$, is also formed. Unlike with the permethylated analogues, however, these reactions proceed smoothly at room temperature (12–24 h). Microcrystalline yellow or green products are obtained in 50–90% yield upon addition of petroleum ether to the reaction mixture. The product in each case is a mixture of endo and exo isomers in almost equal proportions. Although the isomers have proven to be inseparable by physical means, assignment of the ^{1}H NMR resonances of a mixture of the isomers was accomplished through difference NOE and magnetization transfer experiments (see Table II). Difference NOE experiments allowed the correlation of each of the cyclopentadienyl signals with its neighboring vinylic and hydride signals (the phenyl resonances were not well enough resolved to make definite assignments). The magnetization transfer results were then used to unambiguously assign the vinylic and hydride resonances: in the exo isomers the signals for the $=CH_2$ and Nb–*H* protons exhibit exchange, whereas in the endo isomers the $=CH(p\text{-X-}C_6H_4)$ and Nb–*H* protons undergo magnetization transfer.

The ^{1}H NMR spectra of these niobocene complexes (see Table I and Figure 1) are similar to those of their permethylniobocene

(4) Johnson, C. D. *The Hammett Equation*; Cambridge University Press: Cambridge, England, 1973; Chapter 1.
(5) (a) Lowry, T. H.; Richardson, K. S. *Mechanism and Theory in Organic Chemisty*, 2nd ed.; Harper and Row: New York, 1981; pp 197–205. (b) Hammond, G. S. *J. Am. Chem. Soc.* **1955**, *77*, 334–338.
(6) (a) Tebbe, F. N.; Parshall, G. W. *J. Am. Chem. Soc.* **1971**, *93*, 3793–3795. (b) Klazinga, A. H.; Teuben, J. H. *J. Organomet. Chem.* **1978**, *157*, 413–419. (c) Klazinga, A. H.; Teuben, J. H. *Ibid.* **1980**, *194*, 309–316. (d) Eichner, M. E.; Alt, H. G.; Rausch, M. D. *Ibid.* **1984**, *264*, 309–316.
(7) Gibson, V. C.; Bercaw, J. E.; Bruton, W. J., Jr.; Sanner, R. D. *Organometallics* **1986**, *5*, 976–979.
(8) (a) Guggenberger, L. J.; Meakin, P.; Tebbe, F. N. *J. Am. Chem. Soc.* **1974**, *96*, 5420–5427. (b) References 2b and 5. (c) Cohen, S. A.; Auburn, P. R.; Bercaw, J. E. *J. Am. Chem. Soc.* **1983**, *105*, 1136–1143.

Table I. ^{1}H nd ^{13}C NMR Data

Compound	Assignment	δ/ppm (Coupling/Hz) ^{1}H	^{13}C
$Cp^{*}_2Nb(CH_2{=}CHC_6H_4\text{-}m\text{-}CF_3)H$[a,b]	$C_5(CH_3)_5$	1.40(s), 1.56(s)	11.5, 11.2 (q; 120)
	$C_5(CH_3)_5$		105.8(s), 105.3(s)
	Nb-*H*	-2.27(s,br)	
endo-3	H_a	0.30(dd; 13.0, 6.0)	
	H_b	0.14(dd; 10.0, 6.0)	
	H_x	2.19(dd; 10.0, 13.0)	
	$=CH_2$		24.0(t; 146)
	=CHPh		45.0(d; 144)
	C_6H_4	8.00(s)	153.6(s), 126.8(s)
		7.58(d; [c])	133.6(d; 173)
		7.04(t; 8.0)	128.1(d; [c])
		6.82(d; 8.0)	127.5(d; [c])
			118.5(d; 177)
$Cp^{*}_2Nb(CH_2{=}CHC_6H_4\text{-}m\text{-}CH_3)H$[a]	$C_5(CH_3)_5$	1.55(s), 1.72(s)	11.4, 11.2 (q; 126)
	$C_5(CH_3)_5$		105.3, 104.7(s)
	Nb-*H*	-2.23(s,br)	
endo-4	H_a	0.43(dd; 14.0, 6.0)	
	H_b	0.21(dd; 10.0, 6.0)	
	H_x	2.15(dd; 10.0, 14.0)	
	$=CH_2$		24.0(dd; 143)
	=CHPh		46.2(d; 139)
	CH_3	2.38(s)	21.8(q; 125)
	C_6H_4	6.8-7.6[d]	151.1(s), 127.2(s)
			135.9(d; 161)
			131.1(d; 160)
			128.3(d; [c])
			123.1(d; 160)
$Cp^{*}_2Nb(CH_2{=}CHC_6H_4\text{-}m\text{-}NMe_2)H$[a,e]	$C_5(CH_3)_5$	1.54(s),1.65(s)	
	Nb-*H*	-2.26(s,br)	
endo-5	H_a	0.51(dd; 14.0, 6.0)	
	H_b	0.18(dd; 10.0, 6.0)	
	H_x	2.30(dd; 10.0, 14.0)	
	$N(CH_3)_2$	3.05(s)	
	C_6H_4	6.8-7.6[d]	
$Cp_2Nb(CH_2{=}CHC_6H_5)H$[f]	C_5H_5	4.48(s)	94.2(d,quin; 175,7)
	C_5H_5	4.35(s)	93.5(d,quin; 175,7)
	Nb-*H*	-2.41(s,br)	
endo-7	H_a	1.28(dd; 13.0, 5.5)	
	H_b	0.92(dd; 10.1, 5.5)	
	H_x	3.32(dd; 10.1, 13.0)	
	$=CH_2$		13.9(dd; 148,149)
	=CHPh		33.9(d; 143)
	C_6H_5	6.8-7.6[d]	153.6(s)
			127.9(dd; 156,7)
			126.6(d,br; 155)
			122.1(dt; 158,7)
$Cp_2Nb(CH_2{=}CHC_6H_5)H$[f]	C_5H_5	4.52(s)	93.5(d,quin; 175,7)
	C_5H_5	4.25(s)	92.7(d,quin; 175,7)
	Nb-*H*	-2.89(s,br)	
exo-7	H_a	1.62(ddd; 13.1, 6.9, 1.7)	
	H_b	1.45(ddd; 10.0, 6.9, 2.2)	
	H_x	2.58(dd; 10.0, 13.1)	
	$=CH_2$		9.1(td; 151,5)
	=CHPh		35.3(d 142)
	C_6H_5	6.8-7.6[d]	152.8(s)
			127.5(dd; 155,7)
			126.6(d,br; 155)
			121.6(dt; 157,7)
$Cp_2Nb(CH_2{=}CHC_6H_4\text{-}p\text{-}CF_3)H$[b,f]	C_5H_5	4.42(s)	94.6(d,quin; 175,7)
	C_5H_5	4.25(s)	94.0(d,quin; 176,7)
	Nb-*H*	-2.47(s,br)	
endo-8	H_a	1.11(dd; 13.1, 5.8)	
	H_b	0.85(dd; 9.8, 5.8)	
	H_x	3.08(dd; 9.8, 13.1)	
	$=CH_2$		14.1(dd; 146,147)
	=CHPh		33.6(d; 148)
	C_6H_5	6.8-7.6[d]	159.2(s)
			120-130[g]
$Cp_2Nb(CH_2{=}CHC_6H_4\text{-}p\text{-}CF_3)H$[b,f]	C_5H_5	4.45(s)	93.7(d,quin; 176,7)
	C_5H_5	4.13(s)	93.1(d,quin; 175,7)
	Nb-*H*	-2.82(s,br)	
exo-8	H_a	1.44(ddd; 13.0, 9.9, 1.6)	
	H_b	1.37(ddd; 9.9, 6.9, 2.1)	
	H_x	2.36(dd; 9.9, 13.0)	
	$=CH_2$		9.7(dd; 145,146)
	=CHPh		34.3(d; 147)
	C_6H_5	6.8-7.6[d]	158.3(s)
			120-130[g]

Table I (Continued)

Compound	Assignment	δ/ppm (Coupling/Hz) ^{1}H	^{13}C
$Cp_2Nb(CH_2{=}CHC_6H_4\text{-}p\text{-}OMe)H$[f]	C_5H_5	4.48(s)	94.08(d,quin; 176,7)
	C_5H_5	4.37(s)	93.41(d,quin; 176,7)
	Nb-*H*	-2.47(s,br)	
endo-9	H_a	1.25(dd; 13.0, 5.4)	
	H_b	0.94(dd; 10.2, 5.4)	
	H_x	3.34(dd; 10.2, 13.0)	
	OCH_3	3.39(s)	55.04(q; 141)
	$=CH_2$		14.02(t; 150)
	=CHPh		33.38(d; 158)
	C_6H_5	6.8-7.6[d]	155.55(s),145.66(s)
			127.82(d; 155)
			113.42(dd; 157,4)
$Cp_2Nb(CH_2{=}CHC_6H_4\text{-}p\text{-}OMe)H$[f]	C_5H_5	4.52(s)	93.47(d,quin; 176,7)
	C_5H_5	4.28(s)	92.58(d,quin; 176,7)
	Nb-*H*	-2.94(s,br)	
exo-9	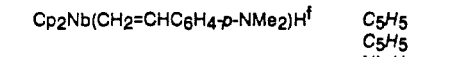 H_a	1.62(ddd; 13.1, 6.8, 1.8)	
	H_b	1.46(ddd; 10.1, 6.8, 2.3)	
	H_x	2.59(dd; 6.8)	
	OCH_3	3.41(s)	55.09(q; 141)
	$=CH_2$		8.77(t; 152)
	=CHPh		34.91(d; 149)
	C_6H_5	6.8-7.6[d]	156.01(s),145.66(s)
			127.82(d; 155)
			113.42(dd; 157,4)
$Cp_2Nb(CH_2{=}CHC_6H_4\text{-}p\text{-}NMe_2)H$[f]	C_5H_5	4.50(s)	93.83(d,quin; 175,7)
	C_5H_5	4.42(s)	93.13(d,quin; 175,7)
	Nb-*H*	-2.43(s,br)	
endo-10	H_a	1.36(dd; 13.0, 5.3)	
	H_b	0.99(dd; 10.3, 5.3)	
	H_x	3.44(dd; 10.3, 13.0)	
	$N(CH_3)_2$	2.61(s)	41.30(q; 134)
	$=CH_2$		14.39(t; 148)
	=CHPh		33.85(d; 149)
	C_6H_5	6.8-7.6[d]	146.62(s),141.70(s)
			127.44(d; 154)
			113.07(d; 154)
$Cp_2Nb(CH_2{=}CHC_6H_4\text{-}p\text{-}NMe_2)H$[f]	C_5H_5	4.55(s)	93.26(d,quin; 175,7)
	C_5H_5	4.35(s)	92.30(d,quin; 175,7)
	Nb-*H*	-2.97(s,br)	
exo-10	H_a	1.73(ddd; 13.1, 6.6, 1.7)	
	H_b	1.52(ddd; 10.1, 6.6, 2.1)	
	H_x	—(dd; 10.1, 13.1)	
	$N(CH_3)_2$	2.63(s)	41.21(q; 134)
	$=CH_2$		9.02(t; 148)
	=CHPh		35.75(d; 147)
	C_6H_5	6.8-7.6[d]	147.01(s),140.78(s)
			127.44(d; 154)
			113.07(d; 154)
$Cp_2Nb(CH_2{=}CHCH_3)H$[g]	C_5H_5	4.58(s)	
	C_5H_5	4.44(s)	
	Nb-*H*	-2.95(s,br)	
endo-16	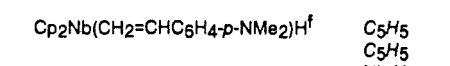 H_a	1.01(dd; 10.2, 4.1)	
	H_b	0.49(dd; 12.1, 4.1)	
	H_x	1.99(dd; 10.2, 12.1)	
	CH_3	1.93(d; 6.4)	
$Cp_2Nb(CH_2{=}CHCH_3)H$[g]	C_5H_5	4.47(s)	
	C_5H_5	4.44(s)	
	Nb-*H*	-3.19(s,br)	
exo-16	H_a	1.45(ddd; 10.1, 5.5, 1.9)	
	H_b	0.85(ddd; 12.3, 5.5, 1.4)	
	H_x	1.24(dd; 10.1, 12.3)	
	CH_3	1.64(d; 6.5)	
$Cp_2Nb(C{=}NCH_3)(N(CH_3)_2)$[a,e]	C_5H_5	5.08(s)	
	$C{=}NCH_3$	2.92(s)	
	$N(CH_3)_2$	2.76(s,br)	
$Cp_2Ta(CH_2{=}CH_2)(CH_2CH_3)$[e,f]	C_5H_5	4.49(s)	
	$=CH_2$	1.11(t; 11.1)	
	$=CH_2$	0.60(t; 11.1)	
	CH_2CH_3	1.32(q; 7.4)	
	CH_2CH_3	1.61(t; 7.4)	

[a] Measured on a JEOL-FX-90Q spectrometer (90 MHz ^{1}H, 23 MHz ^{13}C). [b] The ^{13}C resonance of the CF_3 group was not found. [c] Signal obscured by overlap with the solvent signal. [d] The phenyl region was not resolved. [e] The ^{13}C spectrum was not measured for this compound. [f] The ^{1}H spectrum was measured on a Bruker WM-500 spectrometer (500.13 MHz) in C_6D_6. The ^{13}C spectrum was measured on a JEOL GX-400 spectrometer (100.25 MHz) in dioxane-d_8. [g] The ^{1}H spectrum was measured on a Bruker WM-500 spectrometer (500.13 MHz) in C_6D_6. The high-resolution ^{1}H NMR spectrum has not been previously reported for this compound.

Table II. Assignment of the Endo and Exo Niobocene Styrene Hydride Isomers by NMR Spectroscopy

difference NOE experiments	
signal irradiated	signals showing enhancement
Cp (endo)	Ph, H(endo), H_a(endo)
Cp′ (endo)	H_b(endo), H_x(endo), H(endo)
Cp (exo)	Ph, H(exo), H_a(exo)
Cp′ (exo)	H_b(exo), H_x(exo), H(exo)
magnetization transfer experiments	
signal irradiated	signal effected
H(endo)	=C*H*Ph(endo)
H(exo)	=CH_2(exo)

analogues. At room temperature, the inequivalent Cp rings give rise to two overlapping pairs of singlets for the (η^5-C_5H_5) protons, the signals due to the endo isomer being in between the two signals due to the exo isomer. At 500 MHz the olefinic protons of the endo isomer exist as three sets of doublets of doublets. The =C*H*R resonance of the exo complexes is likewise a doublet of doublets, but the =CH_2 protons show an additional small coupling to the Nb–*H* ($J \approx 2$ Hz). The coupling constants of the olefinic protons are essentially independent of the para substitution, but the geminal coupling constants are consistently different for the exo (≈6.8 Hz) and endo (≈5.5 Hz) isomers. The hydride resonances are broad singlets at about −2.5 to −3.0 ppm, the signal due to the exo isomer always being slightly more upfield. The resonances were too broad to detect the coupling to the vinylic protons.

The feature of most interest in the ^{13}C spectra for these compounds, $^1J_{C-H}$ for the vinylic signals, is in the 145–150-Hz range, suggesting considerable metallacyclopropane character, although not quite as much as for the more electron-rich permethylniobocene system ($^1J_{C-H} \approx 140$–145 Hz), as would be expected on the basis of the relative electron-donating abilities of Cp and Cp*. Infrared and mass spectral data are summarized in the Experimental Section.

Reactions of Olefin Hydride Compounds with Trapping Ligands. The sterically encumbered permethylniobocene olefin hydride compounds were found to react only with small ligands (L = CO and $CNCH_3$) to afford the ligand-trapped alkyl complexes $Cp^*_2Nb(CH_2CH_2R)L$. In contrast, the niobocene complexes react with a larger variety of ligands (L = CO, $CNCH_3$, PMe_3, $P(OMe)_3$, and C_2H_4); however, the predominant products (>90%) arise from substitution of the olefin by the trapping ligands to afford the previously described $Cp_2Nb(H)(L)$ compounds (L = CO,[6a] PMe_3,[6a] $P(OMe)_3$,[9] and C_2H_4[10]). The reaction with $CNCH_3$ is more complex; there appears to be further reaction of the initial reaction product with excess methyl isocyanide. Indeed, it was subsequently found that Cp_2NbH_3 reacts with excess $CNCH_3$ in a closed vessel to give high yields of $Cp_2Nb(CNCH_3)(NMe_2)$. Presumably there is an initial substitution of methyl isocyanide for H_2 to afford an unobserved $Cp_2Nb(H)(CNCH_3)$ species that rapidly reacts with the released hydrogen and another equivalent of $CNCH_3$ to afford the final amide–isocyanide complex.

The permethyltantalocene complexes have been shown to exhibit the same types of steric restrictions found in the permethylniobocene system,[7] as may be expected on the basis of the very similar sizes of Nb and Ta. The tantalocene compounds are more stable than their niobocene analogues and have previously been shown to react with several ligands to form the trapped alkyl species.[11] We have also found that the tantalocene ethylene hydride complex will react with ethylene at elevated temperatures to form the ethylene ethyl complex. This compound has been characterized by proton NMR and found to be similar to the previously described niobocene ethylene ethyl complex.[6a,8a]

(9) Although not previously reported, this compound was assigned by its similarity (^{1}H NMR, C_6D_6) to the trimethylphosphine complex: $\delta_{Cp} = 4.63$ (d, 2 Hz); $\delta_{OMe} = 3.28$ (d, 10.3 Hz); $\delta_H = -7.45$ (d, 33.3 Hz).

(10) In this case a mixture of the ethylene hydride and ethylene ethyl complexes was obtained. See ref 6a and 8a.

(11) (a) Klazinga, A. H.; Teuben, J. H. *J. Organomet. Chem.* **1979**, *165*, 31–37. (b) Klazinga, A. H.; Teuben, J. H. *Ibid.* **1980**, *192*, 75–81.

Table III. Relative Ground-State Energies for Permethylniobocene (Meta-Substituted) Styrene Hydrides

$$Cp^*_2Nb(H_2C{=}CH_2)H + H_2C{=}CHR \xrightleftharpoons{K_{eq},\ 25\ °C} Cp^*_2Nb(H_2C{=}CHR)H + H_2C{=}CH_2$$

R	σ_m	K_{eq}	$\Delta\Delta G°$ [a]
C_6H_4-*m*-CF_3 (**3**)	0.43	0.092 (7)	1.4 (1)
C_6H_5 (**2**)	0.0	0.047 (4)	1.8 (1)
C_6H_4-*m*-CH_3 (**4**)	−0.07	0.063 (10)	1.6 (1)
C_6H_4-*m*-NMe_2 (**5**)	−0.21	0.065 (6)	1.6 (1)

[a] Reported in kcal·mol^{-1}.

Table IV. Relative Ground-State Energies of Niobocene Olefin Hydrides

$$Cp_2Nb(H_2C{=}CHC_6H_5)H + H_2C{=}CHR \xrightleftharpoons{K_{eq},\ 25\ °C} Cp_2Nb(H_2C{=}CHR)H + H_2C{=}CHC_6H_5$$

R	σ_p	K_{eq} [a]	log (K_{eq})	$\Delta\Delta G°$ [b]	rel GSE [b]
p-C_6H_4-CF_3 (**8**)	0.54	17 (2)	1.230 (50)	−1.7 (1)	−1.7 (1)
C_6H_5 (**7**)	0.00	1.0	0.00	0.0	0.0
p-C_6H_4-OMe (**9**)	−0.27	0.29 (4)	−0.544 (60)	0.74 (8)	0.74 (8)
p-C_6H_4-NMe_2 (**10**)	−0.60	0.05 (1)	−1.322 (70)	1.8 (1)	1.8 (1)
CH_3 (**16**)	—	0.0030 (5)	—	3.4 (4)	3.7 (4)

[a] Average of K_{eq}(endo) + K_{eq}(exo). See text for explanation. [b] Reported in kcal·mol^{-1}.

Determination of Ground-State Orderings by Competitive Binding Studies. The relative ground state orderings for the meta-substituted permethylniobocene styrene hydride and the niobocene complexes were determined by carrying out competitive binding experiments:

$$[Nb](CH_2{=}CHC_6H_4\text{-}X)H + CH_2{=}CHR \xrightleftharpoons[25\ °C]{K_{eq}} [Nb](CH_2{=}CHR)H + CH_2{=}CHC_6H_4\text{-}X \quad (4)$$

$$[Nb] = Cp_2Nb;\ X = H,\ p\text{-}CF_3,\ p\text{-}OCH_3,\ p\text{-}NMe_2;\ R = C_6H_5$$

$$[Nb] = Cp^*_2Nb;\ X = H,\ m\text{-}CF_3,\ m\text{-}NMe_2;\ R = H$$

For the meta-substituted styrene hydride complexes of permethylniobocene, as for the para-substituted styrene hydride complexes of permethylniobocene,[2] these experiments were performed by equilibrating the substituted olefin hydride complexes with ethylene. As was found for $Cp^*_2Nb(CH_2{=}CHC_6H_4\text{-}p\text{-}X)H$,[2b] the ground-state energies of the meta-substituted styrene hydride derivatives (**3–5**) of permethylniobocene are insensitive to the nature of the substituent X (Table III).

Equilibration versus ethylene proved unsatisfactory for the normal cyclopentadienyl analogues, since the parent ethylene hydride complex reacts further with excess ethylene.[6a] Thus, the ground-state position for $(\eta^5\text{-}C_5H_5)_2Nb(CH_2{=}CH_2)H$ relative to the other olefin hydride derivatives could not be determined. Performing the equilibrations of the other olefin hydride complexes (*endo*- and *exo*-**7-10** and *endo*- and *exo*-**16**) with styrene results in fairly complicated ^{1}H NMR spectra for these mixtures, but separation of the signals at 500 MHz is sufficient to allow the desired equilibrium data to be determined. The equilibrations were approached from both sides of eq 4 and converged to a single value in each case. In order to avoid decomposition and olefin polymerization, these measurements were carried out at 25 °C, even though the reactions required 2–4 weeks to come to completion.

Importantly, the equilibrium endo:exo isomer ratios for the $Cp_2Nb(CH_2{=}CHR)H$ compounds are found to be insensitive to the nature of the olefin substituent, consistently 1.2–1.4 ($\Delta\Delta G°$ = 0.1–0.2 kcal·mol^{-1}), slightly in favor of the endo isomer. The results of these experiments are summarized in Table IV, the reported K_{eq} actually being the average of K_{eq}(endo) and K_{eq}(exo). It can be readily seen that a sizable ground-state effect is operating for the $[Cp_2Nb]$ styrene hydride complexes, much larger than

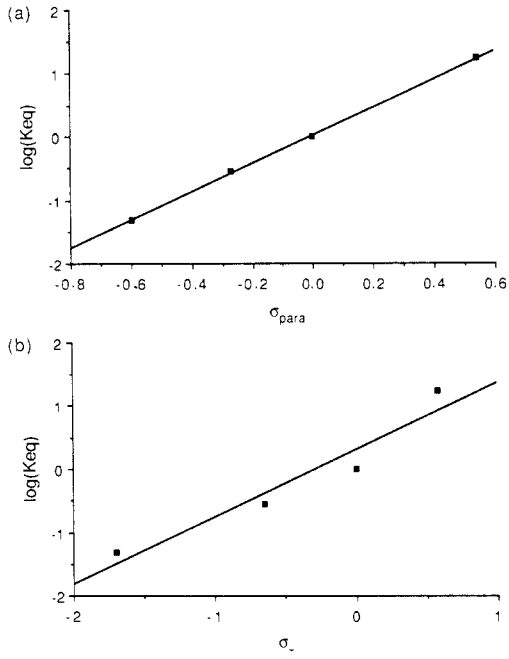

Figure 2. Hammett plot of equilibrium data for *exo*- and *endo*-$Cp_2Nb(H_2C{=}CHC_6H_4\text{-}p\text{-}X)H$ complexes (error bars are on the order of the size of the points): (a) plot of log (K_{eq}) versus σ_p (ρ = 2.2, R = 1.000); (b) plot of log (K_{eq}) versus σ_+ (ρ_+ = 1.1, R = 0.964).

Scheme I

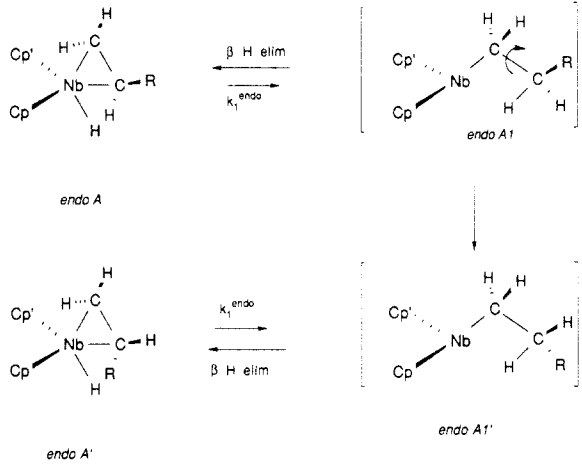

observed for the [Cp^*_2Nb] system. Hammett plots (see Figure 2) of log K_{eq} show a correlation (R = 1.000) with σ_{para} with a $\rho \approx +2.2$, whereas the fit with σ_+ is significantly poorer. In assessing the relative binding abilities for the various olefins it is necessary to account for the free energies of the uncoordinated olefins. By using the free energies of hydrogenation in the previously adopted manner,[2b] the relative ground-state orderings listed in the last column of Table IV were derived. Including the free energies of hydrogenation probably affects only the values for the propene binding constant, since the differences in heats of hydrogenation among the various substituted styrenes are likely to be small relative to the experimental error in K_{eq}.

Determination of the Olefin Insertion Rate by Coalescence and Magnetization Transfer Techniques. The rates of olefin insertion (k_1) for *endo*-$Cp^*_2Nb(CH_2{=}CHC_6H_4\text{-}m\text{-}X)$ (X = CF_3, CH_3, NMe_2) (**3–5**), for *endo*-$Cp_2Nb(CH_2{=}CHCH_3)H$ (**16**), for *endo*-$Cp^*_2Ta(CH_2{=}CHCH_3)H$ (**17**), and for *endo*-$Cp_2Ta(CH_2{=}CHCH_3)H$ (**18**) were determined in a straightforward fashion by using coalescence techniques (^{1}H NMR, 90 MHz). All of these olefin hydride complexes have inequivalent Cp (C_5R_5; R = H, CH_3) rings due to the unsymmetrical substitution of the olefin (e.g., *endo*-A in Scheme I or *exo*-A in Scheme II). As further illustrated in Scheme I the two cyclopentadienyl ring

Scheme II

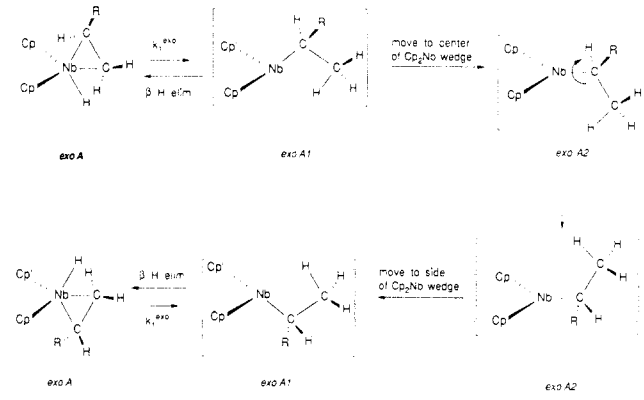

Table V. Rates for Olefin Insertion into the Niobium Hydride Bonds of $Cp^*_2Nb(CH_2{=}CHC_6H_4\text{-}m\text{-}X)H$[a]

X	T (°C)	k_1 (s^{-1})	$\Delta G^\ddagger(T)$[b]	$\Delta G^\ddagger$(50 °C)[c]
H[d] (**2**)	83 (1)	29.5 (10)	18.6 (1)	18.3 (1)
m-CF_3 (**3**)	104 (1)	38.1 (10)	19.6 (1)	19.4 (1)
m-CH_3 (**4**)	76 (1)	26.7 (10)	18.2 (1)	18.0 (1)
m-NMe_2 (**5**)	75 (1)	22.1 (10)	18.3 (1)	18.0 (1)

[a] All data were measured at 90 MHz. [b] Reported in kcal·mol^{-1}. [c] Reported in kcal·mol^{-1}, assuming $\Delta S^\ddagger$ = +7 eu. [d] Data taken from ref 2b.

Table VI. Comparison of $\Delta G^\ddagger$(50 °C)[a] for *endo*-$Cp^*_2Nb(CH_2{=}CHC_6H_4\text{-}p\text{-}X)H$ and *endo*-$Cp^*_2Nb(CH_2{=}CHC_6H_4\text{-}m\text{-}X)H$ Complexes

X	σ_{meta}[b]	$\Delta G^\ddagger$(meta)[c]	σ_{para}[b]	$\Delta G^\ddagger$(para)[c,d]
CF_3	0.43	19.4	0.54	19.4
H	0.00	18.3	0.00	18.3
CH_3	−0.07	18.0	−0.17	18.1
NMe_2	−0.21	18.0	−0.83	17.7

[a] Assuming $\Delta S^\ddagger$ = +7 eu. [b] Data taken from ref 3. [c] $\Delta G^\ddagger$ in kcal·mol^{-1} at 50 °C. [d] Data taken from ref 2b.

Table VII. Insertion Rates for Niobium and Tantalum Propene Hydride Complexes[a]

compound	T (°C)	k_1 (s^{-1})	$\Delta G^\ddagger(T)$[b]
endo-$Cp^*_2Nb(CH_2{=}CHCH_3)H$ (*endo*-**15**)[c]	−1 (1)	25.3 (11)	14.1 (1)
endo-$Cp_2Nb(CH_2{=}CHCH_3)H$ (*endo*-**16**)	45 (5)	30.0 (10)	16.5 (3)
exo-$Cp_2Nb(CH_2{=}CHCH_3)H$ (*exo*-**16**)[d]	75 (5)	7.0 (10)	19.1 (3)
(*exo*-**16**)[e]	37 (1)	2.1 (1)	17.7 (1)
endo-$Cp^*_2Ta(CH_2{=}CHCH_3)H$ (*endo*-**17**)	72 (1)	26.0 (10)	18.1 (1)
endo-$Cp_2Ta(CH_2{=}CHCH_3)H$ (*endo*-**18**)	101 (1)	28.2 (10)	19.6 (1)
exo-$Cp_2Ta(CH_2{=}CHCH_3)H$ (*exo*-**18**)[d]	139 (1)	7.1 (10)	22.8 (1)

[a] Obtained by Cp ring coalescence at 90 MHz unless otherwise noted. [b] Reported in kcal·mol^{-1}. [c] Data taken from ref 2b. [d] Lower limits for k_1 and upper limits for $\Delta G^\ddagger(T)$. See text for explanation. [e] Measured by magnetization transfer from $CH_3CH{=}CH_2$ to [$CH_3CH{=}CH_2$ + TaH].

environments for the endo isomers can be interchanged by olefin insertion to A1, rotation about the C–C single bond of the alkyl to afford A1′, followed by β-H elimination to *endo*-A′. The rate of insertion (k_1^{endo} at the temperature of coalescence, T_c) may be calculated from the frequency separation of the two C_5R_5 resonances in the slow exchange limit[12] and the free energy of activation ($\Delta G^\ddagger(T_c)$) obtained from the Eyring equation. Values for T_c, $k_1^{endo}(T_c)$, $\Delta G^\ddagger(T_c)$, and $\Delta G^\ddagger$(50 °C) for Cp^*_2Nb-

(12) The value of k_1 is, in fact, equal to $2k_{exchange}$ (at all temperatures), since, on average, two k_1 events are required to effect ring site exchange; see Johnson (Johnson, C. S., Jr. *Adv. Magn. Reson.* **1965**, *1*, 33–102 (in particular pp 64–82)) and references therein for discussion of relevant examples. This factor of 2 was not used in the previously reported experiments with *endo*-$Cp^*_2Nb(CH_2{=}CHR)H$ (ref 2). While the conclusions from the previous work are unchanged, using the correct values of k_1 (for the points derived from coalescence experiments) in the Arrhenius plots (Figure 4 and Table IV of ref 2b; Figure 4 of the supplementary material) leads to a better correlation and slight change in $\Delta S^\ddagger$ from −7 (±5) eu to +7 (±5) eu, with the corresponding small changes in $\Delta H^\ddagger$ and $\Delta G^\ddagger$.

Scheme III

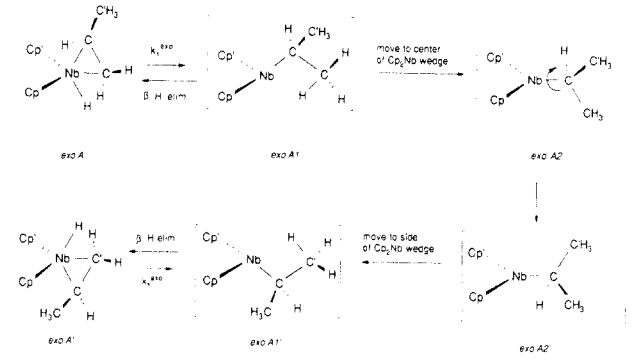

$(CH_2{=}CHC_6H_4\text{-}m\text{-}X)H$ (**3–5**) are given in Table V. Values of $\Delta G^{\ddagger}$(50 °C) were calculated for complexes $Cp^*_2Nb(CH_2{=}CHC_6H_4\text{-}m\text{-}X)H$ (**3–5**), for comparison (Table VI) to the previously reported[2b] para-substituted derivatives, using an average value of +7 (±5) eu for $\Delta S^{\ddagger}$.[12] With use of the coalescence data for cyclopentadienyl ring site exchange, the insertion rate constants (k_1^{endo}) and activation free energies for endo **16–18** were also obtained (Table VII). As can be seen, in each case the tantalum complexes undergo insertion much more slowly than the niobium analogues.

We were unable to use coalescence methods to determine the insertion rate constants for the other olefin hydride complexes. The proton NMR signals of the Cp rings of the endo and exo isomers overlap, making it difficult to determine coalescence. Moreover, the niobocene complexes have much lower thermal stability than the analogous permethylniobocene, tantalocene, or permethyltantalocene derivatives, partially decomposing before the coalescence temperature (>100 °C) can be attained. An additional complication arises in the case of the exo isomers: the rate of exchange of the two cyclopentadienyl ring sites is slower than olefin insertion into the Nb–H bond. As shown in Scheme II, after *exo*-A undergoes olefin insertion the alkyl group of A1 must "swing" to the center of the equatorial plane of the bent sandwich structure (A1 → A2), undergo rotation about the Nb–$CHRCH_3$ bond (A2 → A2′), "swing" to the other side of the wedge (A2′ → A1′), and β-H eliminate in order to exchange Cp sites (*exo*-A → *exo*-A′). Inspection of the results for *exo*-**8** reveals that the barrier of 17 kcal·mol^{-1} for exchange of Nb–*H* with $PhCH{=}CH_2$ by magnetization transfer (vida infra) is considerably less than the ≈19 kcal·mol^{-1} barrier for Cp site exchange (see Table VII). Thus, there appears to be a nonnegligible barrier for passing the Nb(–$CHRCH_3$) group through the center of the wedge and/or rotating about the Nb–C_α bond.

A further complication arises in the calculation of k_1^{exo} by magnetization transfer for the exo propene hydride complexes. Since the methyl groups of the isopropyl ligand, generated by insertion from the exo propene hydride, may be related by a mirror plane (*exo*-A2 and *exo*-A2′, Scheme III), magnetization is exchanged between the Nb—*H*, Nb($CH_2{=}CHCH_3$), and Nb($CH_2{=}CHCH_3$) signals. We can treat this as a two-site exchange system[13] by monitoring the magnetization transfer between [Nb—*H* + Nb($CH_2{=}CHCH_3$)] and Nb($CH_2{=}CHCH_3$). As shown in Scheme III, this still requires the "swinging" process but not a complete rotation (a methyl group does not have to be a full 90° out of the plane of the wedge) to lead to exchange. Qualitatively we see transfer between the Nb—*H* and the Nb($CH_2{=}CHCH_3$) at about the same rate as the exchange into the other methyl group, and this rate is found to be much faster than that for Cp exchange.[14] The insertion rates and barriers for

(13) The quantitative analysis of multiple site magnetization transfer, while possible, is not straightforward. We have not attempted such a treatment. See, for example: Muhandiram, D. R.; McClung, R. E. D. *J. Magn. Reson.* **1987**, *71*, 187–192.

(14) This observation seems to indicate that rotation is the slow step of Cp ring exchange for these exo complexes rather than "swinging" through the center of the wedge; however, this latter process may still contribute slightly to the overall exchange rate.

Table VIII. Rates for Olefin Insertion into the Niobium Hydride Bonds of *exo*- and *endo*-$Cp_2Nb(CH_2{=}CHC_6H_4\text{-}p\text{-}X)H$[a]

compd	X	T (°C)	k_1 (s^{-1})	$\Delta G^{\ddagger}(T)$[b]	k_1 (s^{-1})$^{50°C}$	$\Delta G^{\ddagger}$-(50 °C)[b]
endo-**7**	H	89 (1)	5.6 (2)	20.1 (1)	0.09 (2)	20.5 (1)
endo-**8**	CF_3	101 (1)	3.2 (2)	21.2 (1)	0.01 (1)	21.7 (1)
endo-**9**	OMe	84 (1)	5.3 (3)	19.8 (1)	0.15 (2)	20.2 (1)
endo-**10**	NMe_2	83 (1)	6.6 (4)	19.6 (1)	0.21 (3)	20.0 (1)
exo-**7**[c]	H	25 (1)	2.2 (5)	17.0 (2)		
exo-**7**	H	26 (1)	2.2 (3)	17.0 (1)		
exo-**7**	H	36 (1)	5.9 (3)	17.0 (1)	30 (1)	16.8 (1)
exo-**7**	H	46 (1)	21.1 (20)	16.8 (1)		
exo-**7**	H	52 (2)	36.7 (15)	16.8 (1)		
exo-**8**	CF_3	28 (1)	5.8 (5)	16.6 (1)	58 (6)	16.3 (1)
exo-**8**[d]	CF_3	57 (1)	0.50 (5)	19.4 (1)		
exo-**9**	OMe	36 (1)	4.2 (3)	17.2 (1)	18 (2)	17.1 (1)
exo-**10**	NMe_2	37 (1)	3.2 (2)	17.5 (1)	8.5 (10)	17.6 (1)

[a] All rate constants measured by magnetization transfer on a Bruker WM-500 in C_6D_6 unless otherwise noted. [b] Reported in kcal·mol^{-1}. [c] Measured in DMF-d_7. [d] Rate of Cp exchange measured by magnetization transfer.

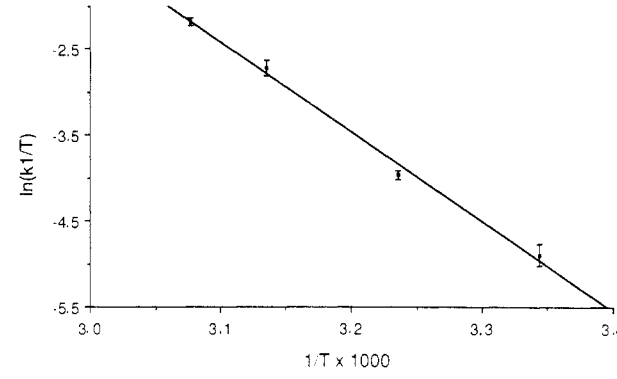

Figure 3. Eyring plot for olefin insertion of *exo*-$Cp_2Nb(H_2C{=}CHC_6H_5)H$: $\Delta H^{\ddagger}$ = 20.7 kcal·mol^{-1}, $\Delta S^{\ddagger}$ = +12 eu, and R = 0.997.

exo-$Cp_2Nb(H)(CH_2{=}CHCH_3)$ and *exo*-$Cp_2Ta(H)(CH_2{=}CHCH_3)$ are listed together with the data for the endo isomers in Table VII, but for the reasons stated above, they represent lower limits for k_1^{exo} and upper limits for $\Delta G^{\ddagger}$. The rate constants for Cp site exchange for the endo propene hydride derivatives (like the endo styrene hydride derivatives) are, however, simply $^1/_2 k_1^{endo}$.

The rates of olefin insertion (k_1) for both endo and exo isomers of the niobocene styrene hydride complexes (**7–10**) were successfully determined by magnetization transfer experiments (^{1}H NMR, 500 MHz), and the results are summarized in Table VIII. Applications of this method to the closely related $Cp^*_2Nb(CH_2{=}CHR)H$ systems have been described previously.[2] A difference NOE experiment was performed for $Cp_2Nb(CH_2{=}CHC_6H_5)H$ at −10 °C (where magnetization transfer is slow) in order to verify that the NOE enhancement between the exchanging sites was negligibly small. The various vinylic and hydride signals were selectively irradiated, and no detectable NOE was found to occur between the hydride and the vinylic protons, although there was some enhancement observed between the various vinylic signals and between the vinylic and cyclopentadienyl signals. These results suggest that the magnetization transfer data are not complicated by competing exchange and NOE effects. Moreover, this method allowed the determination of the rate constants at much lower temperatures (25–100 °C) than the coalescence procedure and thus lessened the problem of sample decomposition. The activation parameters for the insertion reaction of the *exo*-$Cp_2Nb(CH_2{=}CHC_6H_5)H$ were determined over the temperature range 27–52 °C. An Eyring treatment of these data (Figure 3) yields $\Delta H^{\ddagger}$ = 20.7 (7) kcal·mol^{-1}, $\Delta S^{\ddagger}$ = +12 (2) eu, with $\Delta G^{\ddagger}$(50 °C) = 16.8 (1) kcal·mol^{-1}. As was found for the permethylniobocene compounds (+7 ± 5 eu),[2,11] the $\Delta S^{\ddagger}$ value is fairly small. In normalizing rate constants to a standard temperature (50 °C for comparison[2b]), the assumption has been made that $\Delta S^{\ddagger}$ = +7 (±5) eu for all compounds.[12]

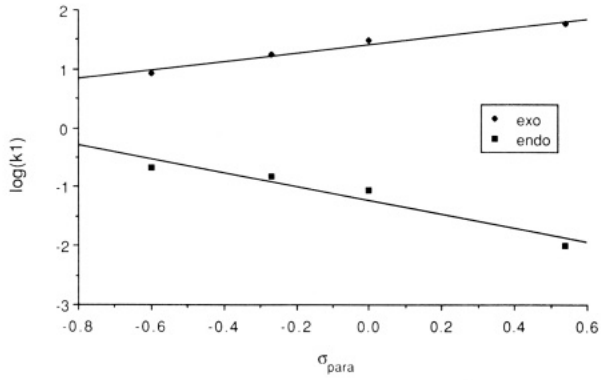

Figure 4. Hammett plots of the olefin insertion rates of *exo*- and *endo*-$Cp_2Nb(H_2C{=}CHC_6H_4\text{-}p\text{-}X)H$ versus σ_p (error bars are on the order of the size of the points): ρ(exo) = 0.72, R = 0.986; ρ(endo) = −1.06, R = 0.966.

Scheme IV

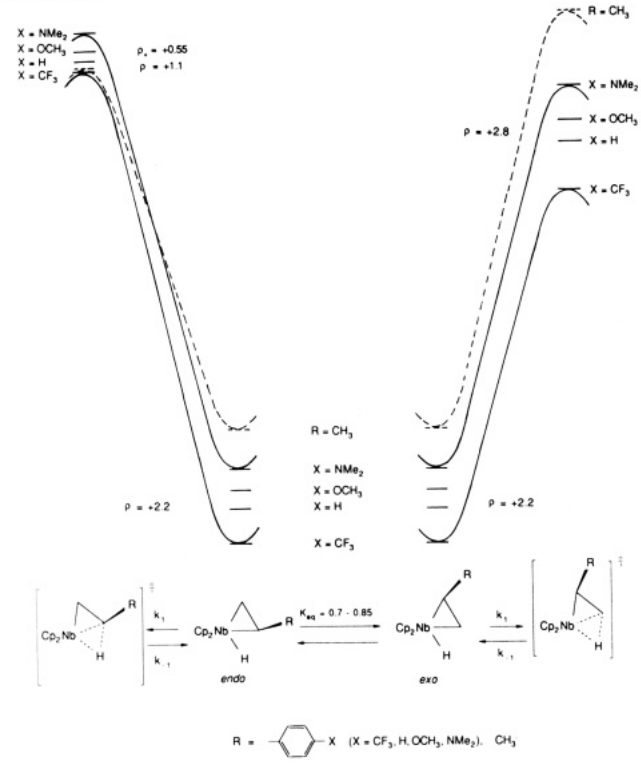

The exo styrene hydride isomers are found to have much lower barriers to insertion (consistently 3–5 kcal·mol^{-1} less) than the corresponding endo isomers. Hammett plots of the rate data for the para-substituted styrene hydride derivatives show reasonable correlations with σ_{para} for both isomers (Figure 4), although the correlation for the endo derivatives is noticeably curved. The endo isomers exhibit faster rate constants with electron-releasing substituents (ρ = −1.1, R = 0.966), while for the exo derivatives the rate increases systematically as the electron-withdrawing power of the substituent increases (ρ = 0.7, R = 0.986). By combining the equilibrium olefin binding data, which orders the ground states, with the kinetic data, the relative energies of the transition states can be derived (Scheme IV). Again, the exo levels show a good correlation with σ_p with a ρ value of +2.8 (R = 0.996); however, the endo levels correlate quite well with σ_+ (ρ_+ = 0.55, R = 0.994),[15] thus explaining why the endo rate data do not correlate particularly well with either σ_{para} or σ_{plus} (the ground states correlate with σ_{para} and the transition states with σ_{plus}).

(15) To the extent that the phenyl ring is in direct resonance with the incipient β carbon (but not the α carbon) in the transition state, σ_+ should correlate better than σ_p for the endo styrene hydride complexes, and σ_p should correlate better than σ_+ for the exo styrene hydride complexes. This is, in fact, the case.

Table IX. Olefin Insertion Rates for Niobium and Tantalum Ethylene Hydride Complexes

compound	T (°C)	k_1 (s^{-1})	$\Delta G^{\ddagger}(T)^a$
$Cp_2Nb(CH_2{=}CH_2)H$ (**11**)	33 (1)	2.8 (3)	17.3 (1)
	45 (1)	9.3 (3)	17.2 (1)
$Cp^*_2Nb(CH_2{=}CH_2)H^b$ (**12**)	50 (1)	2.6 (2)	18.3 (1)
$Cp_2Ta(CH_2{=}CH_2)H$ (**13**)	74 (1)	1.0 (1)	20.4 (1)
$Cp^*_2Ta(CH_2{=}CH_2)H$ (**14**)	100 (1)	2.4 (1)	21.3 (1)

^{a} Reported in kcal·mol^{-1}. ^{b} Data taken from ref 2b.

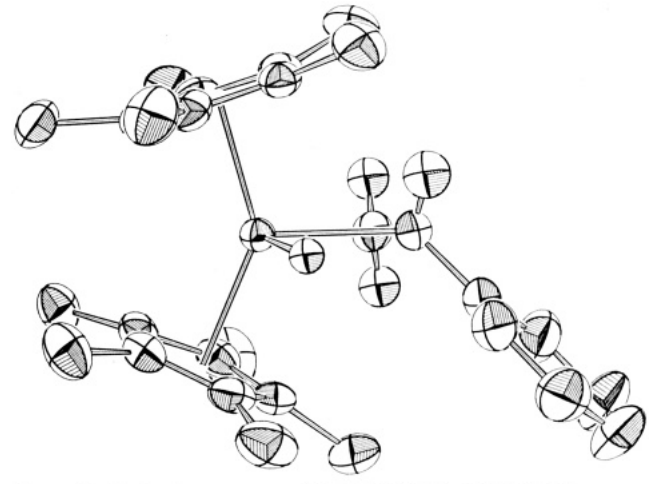

Figure 5. Molecular structure of $Cp^*_2Nb(H_2C{=}CHC_6H_5)H$.

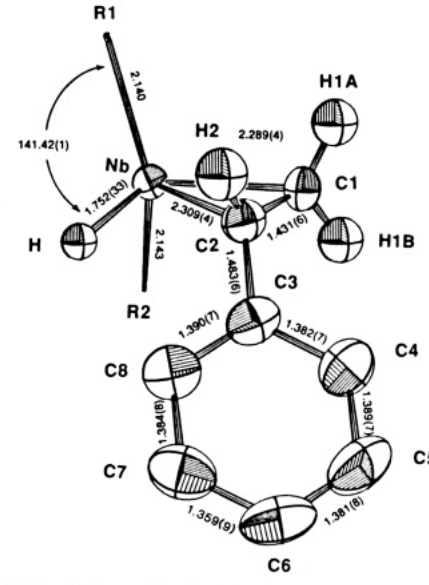

Figure 6. Skeletal view of $Cp^*_2Nb(H_2C{=}CHC_6H_5)H$. Bond distances are in Å and bond angles are in deg.

The insertion rate of the permethylniobocene styrene hydride was measured in several solvents in the initial study and no determinable solvent effect was observed.[2b] A magnetization transfer measurement in DMF-d_7 (the most polar solvent compatible with these compounds) was performed for *exo*-$Cp_2Nb(CH_2{=}CHC_6H_5)H$. At 25 °C the insertion rate in this solvent was found to be identical, within experimental error, with that measured in benzene. Although a complete analysis has not been performed, these results suggest that there can be only a very small solvent effect on the olefin insertion process for these systems.

The results for the ethylene hydride derivatives **11**–**14** are given in Table IX. The tantalum complexes undergo insertion more slowly than the niobium complexes, whereas the (η^5-C_5H_5) derivatives insert more readily than do the (η^5-C_5Me_5) analogues. As might be expected, the ethylene complexes exhibit a rate

intermediate between the extremes set by the endo and exo styrene hydride derivatives.

X-ray Crystal Structure of $Cp^*_2Nb(CH_2{=}CHC_6H_5)H$ (2). A yellow crystal of **2**, suitable for X-ray diffraction, was grown from a slowly cooled petroleum ether/benzene solution. The molecular structure of $Cp^*_2Nb(CH_2{=}CHC_6H_5)H$ is shown in Figure 5; a skeletal view of the niobium coordination sphere with notable bond lengths and angles is shown in Figure 6. The Cp* ligands are coordinated in the conventional η^5 fashion; the Nb–C and C–C bond lengths (Table XII) are similar to those reported for other group V pentamethylcyclopentadienyl complexes.[16] It is evident that the olefin is substituted in the endo position C(2) (Figure 5), confirming the isomeric assignment based on NMR data.[2]

The olefinic carbon–carbon bond length (C(1)–C(2)) of 1.431 (6) Å is larger than that of a free olefin (e.g., ethylene, 1.337 (2) Å[17]) and representative of the C–C distances observed in olefin adducts of low-valent, electron-rich metal centers (e.g., $Cp^*_2Ti(CH_2{=}CH_2)$,[8c] 1.438 (5) Å; $Cp^*Ta(CHCHMe_3)(\eta^2\text{-}C_2H_4)(PMe_3)$,[16c] 1.477 (4) Å; $Cp_2Nb(CH_2{=}CH_2)CH_2CH_3$,[8a] 1.406 (13) Å; $Cp^*_2Ta(CH_2{=}CH_2{\cdot}AlEt_3)H$,[16d] 1.44 (2) Å). The relatively long C=C bond for these structures is indicative of substantial back donation from the metal to the olefin. Overlap of the filled $[Cp^*_2Nb]$ $1a_1$ orbital of **2** with the empty olefin π^* orbital of styrene introduces considerable metallacyclopropane, Nb(V), character into the formally Nb(III) olefin adduct.

The hydride was located in this structure. The Nb–H distance of 1.75 (3) Å compares to other niobium complexes containing terminal hydride ligands (e.g., Cp_2NbH_3,[18] 1.65 (6), 1.76 (7) Å; $[HNb(C_5H_5)(C_5H_4)]_2$,[19] 1.70 (3) Å; and the Ta–H bond distances in Cp_2TaH_3,[18] 1.769 (8), 1.775 (9), and 1.777 (9) Å). A β agostic C–H interaction is ruled out by the long H–C(2) distance of 2.37 Å.

The conformation of the coordinated styrene provides an explanation for the insensitivity of the styrene binding constant to the π releasing or withdrawing power of the para substituent. The phenyl ring of the styrene is indeed twisted away from coplanarity with the olefinic carbons. The dihedral angle between the olefin plane (plane defined by C(1), C(2), and C(3)) and the aromatic ring (C(3)–C(8)) is 32 (9)°. The resulting orientation of the phenyl ring appears to minimize the steric (repulsive) interactions with (η^5-C_5Me_5) methyl groups at the expense of a decrease in the resonance stabilization.

Discussion

Olefin Insertion in the Permethylniobocene Styrene Hydride System. These new data for the meta-substituted styrene hydride complexes of permethylniobocene provide further support for the model suggested earlier:[2b] (i) a ground-state orientation for the phenyl ring (Figure 6) such that the electronic effects of the substituents are *not* transmitted to the Nb–olefin π bonding, and (ii) a four-center transition state for the olefin insertion reaction with a small positive charge developed at the β carbon (ρ_{meta} = −1.2). As was found for the para-substituted styrene hydride complexes of permethylniobocene,[2b] the equilibrium binding constant is insensitive to the nature of the styrene meta substituent (Table III). Electronic effects are exerted only on the transition state: electron-donating groups ($\sigma_{meta} < 0$; CH_3, NMe_2) stabilize the transition state and facilitate the insertion process (relative to H); electron-withdrawing groups ($\sigma_{meta} > 0$; CF_3) retard the insertion process. The value of ΔG^*(50 °C) for the *m*-CF_3 and *p*-CF_3 is essentially the same, supporting the conclusions of others[20] that CF_3 is strongly electron withdrawing by induction, transmitting very little electronic effect through the π orbitals. Since the inductive effect of a substituent is similar at the meta and para positions,[4] this result was anticipated. Similarly, the barriers for insertion for the *m*- and *p*-CH_3 styrenes are essentially the same. Thus, when a substituent exerts its electronic effect primarily through induction, the insertion rates for meta- and para-substituted styrenes are observed to be the same.

Since the NMe_2 group is moderately electron withdrawing by induction, yet strongly electron releasing by resonance, the comparison of the relative rates of insertion for the $CH_2{=}CHC_6H_4$-*m*-NMe_2 and $CH_2{=}CHC_6H_4$-*p*-NMe_2 hydride complexes is particularly revealing. The resonance electronic effect in the transition state is evident when the data for these two complexes are compared: ΔG^* (kcal·mol^{-1} at 50 °C) = 18.0 (1) and 17.7 (1) for *m*-NMe_2 and *p*-NMe_2, respectively. Thus, resonance stabilization is slightly greater than inductive destablization of positive charge at C_β in the transition state. The significance of this result stems from the very nature of the resonance interaction. In order to transfer the electronic effect from the phenyl π orbitals, the phenyl ring must be oriented perpendicular to the p orbital of the C_β. Thus, the results of the X-ray crystal structure determination for $Cp^*_2Nb(CH_2{=}CHC_6H_5)H$ and these new kinetic data for the meta-substituted styrene hydride complexes, particularly for $Cp^*_2Nb(CH_2{=}CHC_6H_4\text{-}p\text{-}NMe_2)H$ versus $Cp^*_2Nb(CH_2{=}CHC_6H_4\text{-}m\text{-}NMe_2)H$, clearly support our earlier proposal that on approach to the transition state the phenyl ring twists (at least partially) back into conjugation with the olefin.

Relative Rates of Insertion for Permethylmetallocene and Metallocene Ethylene and Propene Hydride Complexes of Niobium and Tantalum: Sterics versus Electronics. Comparison of the rate constants (k_1) for insertion among the four ethylene hydride complexes $(C_5R_5)_2M(H)(H_2C{=}CH_2)$ (R = H, CH_3; M = Nb, Ta) highlights the magnitude of electronic effects within this family of compounds (Table IX). A smooth progression for k_1 is observed: $[Cp_2Nb] > [Cp^*_2Nb] > [Cp_2Ta] > [Cp^*_2Ta]$. This trend is readily accommodated by considering the insertion reaction as a reductive process: the formally M(V) metallacyclopropane hydride being converted to the M(III) alkyl intermediate. NMR and structural data for these compounds do indeed indicate substantial metallacyclopropane (vis-ã-vis M(III) olefin adduct) character in the ground state. Hence, the faster rate for the (η^5-C_5H_5) complexes as compared with the corresponding (η^5-C_5Me_5) complexes is attributable to increased stabilization of the ground state by the better donor ability of the latter. Similarly, replacement of Nb (4d metal) by Ta (5d metal) stabilizes M(V) relative to the M(III), again lowering the ground-state energy relative to the transition state, according to the Hammond principle.[5]

The importance of steric destabilization of the ground state relative to the transition state is readily appreciated by comparing the results for the family of endo propene complexes (Table VII). Again the tantalum compounds have considerably larger barriers than their niobium analogues due to increased stability of Ta(V) versus Ta(III) relative to Nb(V) versus Nb(III). Significantly, the order reverses from that seen for the ethylene complexes when the Cp versus Cp* comparison is made; the more electron releasing pentamethylcyclopentadienyl compounds show lower barriers to insertion by about 1–2 kcal·mol^{-1}. Larger steric interactions for the ground state versus alkyl tautomer (and thus the transition state[5]) must be responsible for this reversal. Although the methyl group is expected to be bent back away from the metal in the ground state (cf. the phenyl group for the styrene hydride complex, Figure 6), the propyl tautomer (and hence transition state) is clearly less sterically congested, so that sterics are expected to

(16) (a) Mayer, J. M.; Wolczanski, P. T.; Santarsiero, B. D.; Olson, W. A.; Bercaw, J. E. *Inorg. Chem.* **1983**, *22*, 1149–1155. (b) Messerle, L. W.; Jennishche, P.; Schrock, R. R.; Stucky, G. *J. Am. Chem. Soc.* **1980**, *102*, 6744–6752. (c) Schultz, A. S.; Brown, R. K.; Williams, J. M.; Schrock, R. R. *J. Am. Chem. Soc.* **1981**, *103*, 169–176. (d) Gibson, V. C.; McDade, C.; Santarsiero, B. D.; Bercaw, J. E. *Organometallics* **1988**, *7*, 1.

(17) Bartell, L. S.; Roth, E. A.; Hollowell, C. D.; Kuchitzu, K.; Young, J. E. *J. Chem. Phys.* **1965**, *42*, 2683–2686.

(18) Wilson, R. D.; Koetzle, T. F.; Hart, D. W.; Kvick, A.; Tipton, D. L.; Bau, R. *J. Am. Chem. Soc.* **1977**, *99*, 1775–1781.

(19) (a) Guggenberger, L. J.; Tebbe, F. N. *J. Am. Chem. Soc.* **1971**, *93*, 5924–5925. (b) Guggenberger, L. J. *Inorg. Chem.* **1973**, *12*, 294–301.

(20) There is a small electron-withdrawing effect by resonance of the CF_3 group (delocalization of the negative charge over all three *F*'s). The ratio of the resonant effect to the inductive effect for the CF_3 group has been determined to be 0.29. See: Swain, C. G.; Lupton, Jr., E. C. *J. Am. Chem. Soc.* **1968**, *90*, 4328–4337.

accelerate insertion for the permethylmetallocene derivatives. The much lower binding constant for propylene relative to ethylene[2] in the permethylniobocene system is also likely to be largely a consequence of these unfavorable steric interactions between the methyl group and a (η^5-C_5Me_5) ligand. Although the electronic effects operating in the ethylene system are almost certainly acting here also, the steric effects of the bulky Cp* rings appear to override them for the propene hydride series. The magnitude of these effects suggests that it should be possible to modify the selectivity of systems of this type by playing off electronic and steric interactions.

Kinetic and Thermodynamic Analysis of the Niobocene Styrene Hydride System. Our previous work attempted to detail the electronic effects that are operating in the styrene hydride insertion mechanism for the permethylniobocene system. It was found, however, that sterics moderated the electronic effects, and the linear free energy correlation indicated a ρ of only −0.64.[2b] The results described above for the ethylene and propylene complexes help to document the relative importance of steric and electronic effects at the transition-metal center, but the effects originating from the olefin are not readily apparent. The para-substituted styrene hydride complexes of bis(cyclopentadienyl)niobium provide an almost ideal system in which to study electronic effects associated with the olefin. Since both exo and endo isomers are obtained in nearly equal proportions, steric interactions must be of much less consequence, and electronic effects are expected to be prominent. This feature also allowed us to probe the electronic effects at the α as well as the β carbon of the coordinated olefin.

The relative ground-state energies of the various niobocene styrene hydride complexes have been measured by competitive equilibrium binding and are summarized in Table IV. Whereas the ground-state energies for the permethylniobocene styrene compounds are essentially invariant to meta or para substitution, the niobocene system shows a strong dependence on the para substituent, giving a very linear plot of log K_{eq} versus σ_{para} with a substantial ρ value of +2.2. The positive value of ρ is as anticipated, since more π-acidic olefins (those with electron-withdrawing substituents) are expected to form more stable adducts. The exo to endo isomer ratio is almost invariant to substitution, indicating little steric or electronic preference for α or β substitution. The magnitude of these effects suggests that the phenyl ring is likely in resonance with the Nb–olefin bond for the less crowded (η^5-C_5H_5) complexes. The fact that there is a better correlation with σ_{para} than σ_+ could arise from the high degree of metallacyclopropane character for the niobium olefin bond.

The olefin insertion kinetics for the *endo*-$Cp_2Nb(H)(CH_2{=}CHC_6H_4$-*p*-X) complexes were measured by magnetization transfer techniques and are summarized in Table VIII. Qualitatively these results are similar to those found in the analogous permethylniobocene system: electron-releasing substituents increase the insertion rate. The rate data show a rough correlation[21] with σ_{para} with a ρ value of −1.1, approximately double that found for the [Cp^*_2Nb] system. Without the rigid steric demands, the electronic effects seem more able to exert themselves. On closer analysis some important differences become evident, however. Considering both the competitive binding and rate data, the transition-state orderings can be obtained, giving the energy diagram shown in Scheme IV. The relative orderings of the transition-state energies for the endo derivatives are reversed from those that might be expected by comparing only the relative insertion rates and from those found for the permethylnioboene system.[2] This curious feature likely arises from a competition between ground-state and transition-state effects. Since the transition state appears to be essentially nonpolar, the stabilization of the positive charge buildup on the β-carbon would be expected to be relatively minor and thus unable to overcome the other effects. A Hammett plot of the transition-state data shows a linear correlation with σ_+, further suggesting that for the [Cp_2Nb] system the phenyl ring and the olefin π system can come into complete resonance in the transition state for the endo derivatives.

The insertion rates for the *exo*-$Cp_2Nb(H)(CH_2{=}CHC_6H_4$-*p*-X) complexes were also measured by magnetization transfer and are summarized in Table VIII. Interestingly, these compounds exhibit much lower insertion barriers than the corresponding endo isomers. Plots of log k_1 correlate with σ_{para} and give a ρ value of +0.7:electron-withdrawing substituents accelerate the insertion process. Plotting the transition-state energy levels reveals that they are well separated and correlate with σ_{para} (ρ = +2.8). It appears that, in this case, the ground-state and transition-state effects are working in concert and thus are additive (2.2 + 0.7 = 2.9, very close to the observed value of 2.8). The rather poor correlation with σ_+ in this case could indicate unfavorable steric interactions between the phenyl ring at C_α and a Cp ligand for [Cp_2Nb–$CH(C_6H_4X)(CH_3)$], although the rather small preference ($\leq$0.2 kcal·mol^{-1}) for the endo isomers suggests that steric interactions are *not* dominating the insertion process for the exo or endo complexes in the niobocene system.

These data indicate the following electronic effects are operating: (i) electron-withdrawing substituents at either C_α or C_β stabilize the ground state and increase the olefin binding constant, (ii) electron-releasing substituents at C_β accelerate the insertion process by stabilizing the modest positive charge buildup at this position, (iii) electron-withdrawing substituents at C_α accelerate the insertion process. The origin of the third effect is not entirely clear. Consideration of the energy surface for the insertion reveals that there is a net increase in the Nb–C_α bonding with the transition state more closely resembling the [Cp_2Nb–$CH(C_6H_5)(CH_3)$] tautomer. Electron-withdrawing groups should enhance the ionic character of the Nb–C bonding and increase the bond strength accordingly. Alternatively, there could be negative charge buildup at C_α, which is stabilized by the electron-withdrawing substituents. The distinction between these two possibilities is not sharp; however, we tend to favor the picture based on relative bond strengths. The magnitude of the kinetic ρ's (−1.1 for the endo and +0.7 for the exo isomers) indicates only a modest amount of charge development in the transition state. Moreover, the reaction rates for both the permethylniobocene and niobocene systems are not enhanced in polar solvents as would have been expected for a highly charged transition state.

In comparing the effects of alkyl and aryl groups on the rate constants and ground-state orderings, the aryl group appears to generally be functioning as electron withdrawing (sp^2-hybridized C) relative to the methyl group (sp^3-hybridized C). If C_β did approach the limit of a tricoordinate carbocation in the transition state, one would expect the endo styrene hydride complex to undergo insertion much faster than the propene hydride complex, since the benzylic carbonium ion is much more stable than a secondary carbonium ion.[22] However, neither of these two limiting features is achieved in the transition state for olefin insertion for these group 5 metallocene systems: the magnitude of ρ indicates relatively little positive charge development, and the coordination number of C_β approaches four, not three ($C_\beta \rightarrow sp^3$ hybridization), in the transition state. Thus, the full extent of resonance stabilization of the carbonium ion normally afforded by the phenyl substituent is not available in the bridged ([Nb···H···C_β]) transition state. Inductive destabilization by phenyl further contributes to slowing the rate of insertion for the styrene hydride complex. A similar reversal of effects for phenyl versus methyl has been noted previously for electrophilic attack at olefins proceeding via a bridged transition state.[23]

The electronic effects observed for the *endo*- and *exo*-$Cp_2Nb(CH_2{=}CHC_6H_4$-*p*-X)H compounds are strikingly similar to those reported by Halpern and Okamoto for insertion of styrenes

(21) The line obtained is fairly curved, however. Apparently differing degrees of resonance stabilization are operating for the ground and transition states; the ground states correlate best with σ whereas the transition states correlate best with σ_+.

(22) Wolf, J. F.; Staley, R. H.; Koppel, M.; Taagepera, R. T.; McIver, R. T., Jr.; Beauchamp, J. L.; Taft, R. W. *J. Am. Chem. Soc.* **1974**, *96*, 7552–7554.

(23) Schmidt, G. H.; Garratt, D. G. *The Chemistry of Double-Bonded Functional Groups, Part 2*; Patai, S., Ed.; John Wiley and Sons: New York, 1977; Chapter 9.

into Rh–H bonds.[18] These authors found a smaller ground-state substituent effect ($\rho = +1.0$) and a similar substituent effect on the rate of insertion ($\rho = -0.9$). Although the direction of insertion was not established for this system, the opposing electronic effects are as we find for the *endo*-$Cp_2Nb(CH_2{=}CHC_6H_4\text{-}p\text{-}X)H$ series of complexes, suggesting that $[(PPh_3)_2(H)RhCH_2CH_2C_6H_4X]$ rather than $[(PPh_3)_2(H)RhCH(CH_3)C_6H_4X]$ is the insertion product.

Experimental Section

General Considerations. All manipulations of air-sensitive materials were carried out with glovebox or high vacuum line techniques. Solvents were dried over $LiAlH_4$ or sodium benzophenone and stored over titanocene. Benzene-d_6 and toluene-d_8 were dried over activated 4 Å molecular sieves and stored over titanocene. 1,4-Dioxane-d_8 was also dried over sieves but stored over sodium benzophenone. Dimethylformamide-d_7 (DMF-d_7) was dried and stored over activated alumina. Argon was purified by passage over MnO on vermiculite and activated molecular sieves.

NMR spectra were recorded on Varian EM-390 (^1H, 90 MHz), JEOL FX90Q (^1H, 89.56 MHz; ^{13}C, 22.50 MHz; ^{19}F, 84.26 MHz), JEOL GX400Q (^1H, 399.78 MHz; ^{13}C, 100.38 MHz), and Bruker WM500 (^1H, 500.13 MHz) spectrometers. Infrared spectra were recorded on a Beckman 4240 spectrometer and peak positions are reported in cm^{-1}. All elemental analyses were conducted by L. Henling of the Caltech Analytical Laboratory.

Starting Materials. Styrene (Aldrich), *m*-methylstyrene (Alfa), *p*-methoxystyrene (Aldrich), and ethylmagnesium chloride and *n*-propylmagnesium bromide in diethyl ether solution (Aldrich) were used without further purification. *p*-(Trifluoromethyl)styrene and *p*-(dimethylamino)styrene were prepared as described previously.[2b] *m*-(Trifluoromethyl)styrene was prepared by the literature method for its para-substituted analogue[24] except that the secondary alcohol, $m\text{-}CF_3C_6H_4CH(OH)CH_3$, was formed by the reaction of CH_3MgBr and $m\text{-}CF_3C_6H_4CHO$ (Marshallton). *m*-(Dimethylamino)styrene was prepared by this same procedure except that the secondary alcohol, $m\text{-}NMe_2C_6H_4CH(OH)CH_3$, was prepared by alkylating $m\text{-}NMe_2C_6H_4CO_2H$ (Aldrich) with MeLi (Aldrich) and then reducing the resultant ketone, $m\text{-}NMe_2C_6H_4COCH_3$, with $NaBH_4$ in ethanol. *m*-(Dimethylamino)styrene and *m*-(trifluoromethyl)styrene were purified by vacuum distillation and characterized by ^1H NMR.

$Cp^*_2NbH_3$[25] (**1**), $Cp^*_2Nb(CH_2{=}CHC_6H_5)H$[2b] (**2**), $Cp_2Nb(CH_2{=}CHCH_3)H$[6c] (**16**), and $Cp_2Ta(CH_2{=}CHCH_3)H$[6b] (**18**) were prepared by literature methods. $Cp_2Nb(CH_2{=}CH_2)H$ (**12**) and $Cp_2Ta(CH_2{=}CH_2)H$ (**13**) were prepared by the method previously reported for Ta[6d] except that the reactions were carried out under argon rather than ethylene to prevent formation of the $Cp_2M(CH_2{=}CH_2)(CH_2CH_3)$ complexes. Cp_2NbCl_2 and Cp_2TaCl_2 were prepared by using the trialkyltin reagent as reported by Green[26] and purified by Soxhlet extraction into methylene chloride. The published procedure was followed for the synthesis of Cp_2NbH_3[27] (**6**) from Cp_2NbCl_2 and $LiAlH_4$, the product being purified by sublimation (60–70 °C, 10^{-3} Torr). The syntheses of $Cp^*_2Ta(CH_2{=}CHCH_3)H$ (**17**) and $Cp^*_2Ta(CH_2{=}CH_2)H$ (**14**) from $Cp^*_2TaCl_2$ and the appropriate Grignard reagent (*n*-propyl and ethyl, respectively) have recently been developed in our laboratory.[7]

$Cp^*_2Nb(CH_2{=}CHC_6H_4\text{-}m\text{-}CF_3)H$ (3). *m*-(Trifluoromethyl)styrene (1.0 mL) was added to $Cp^*_2NbH_3$ (**1**) (0.5 g, 1.36 mmol) in 10 mL of toluene. The reaction mixture was heated at 80 °C for 20 h. Toluene was removed under reduced pressure leaving a dark brown oil. Addition of petroleum ether caused a yellow solid to precipitate from solution. Recrystallization from petroleum ether resulted in 360 mg of a yellow crystalline solid (**3**) (49%) ^{19}F NMR (benzene-d_6): δ-62.3 (relative to $CFCl_3$). IR (Nujol): 2715, 1745, 1668, 1594, 1578, 1470, 1378, 1348, 1320, 1212, 1167, 1128, 1108, 1063, 1020, 895, 797, 768, 738, 700, 656. Anal. Calcd for $C_{29}H_{38}F_3Nb$: C, 64.92; H, 7.14. Found: C, 65.01; H, 7.06.

$Cp^*_2Nb(CH_2{=}CHC_6H_4\text{-}m\text{-}CH_3)H$ (4). The same procedure was used as described above except that *m*-methylstyrene (0.7 mL) was added to **1** (0.5 g, 1.36 mmol) in 10 mL of toluene. Yellow crystalline **4** (450 mg) was isolated after petroleum ether recrystallization (68%). IR (Nujol): 2708, 1752, 1688, 1594, 1572, 1486, 1478, 1377, 1280, 1243, 1176, 1152, 1089, 1061, 1022, 896, 880, 792, 768, 734, 698.

$Cp^*_2Nb(CH_2{=}CHC_6H_4\text{-}m\text{-}NMe_2)H$ (5). The same procedure was used as described above except that *m*-(dimethylamino)styrene (0.5 mL) was added to **1** (0.367 g, 1.0 mmol) in 10 mL of toluene. Yellow crystalline **5** (405 mg) was isolated after petroleum ether recrystallization (80%). Anal. Calcd for $C_{30}H_{43}NNb$: C, 77.72; H, 9.57; N, 3.02. Found: C, 77.09; H, 9.37; N, 3.49.

$Cp_2Nb(CH_2{=}CHC_6H_5)H$ (7). Styrene (1 mL, 9 mmol) was syringed into a toluene solution of **6**, Cp_2NbH_3 (0.782 mg, 3.5 mmol), against an argon counterflow at room temperature. After the mixture was stirred overnight (12–24 h) at 25 °C, the resulting orange-yellow solution was filtered and 994 mg (88%) of yellow microcrystalline **7** (≈1:1 mixture of endo and exo isomers) isolated by slow precipitation with petroleum ether. IR (Nujol): 3111, 3093, 3072, 3032, 1727, 1589, 1566, 1489, 1433, 1365, 1298, 1287, 1222, 1176, 1149, 1118, 1075, 1069, 1016, 1008 898, 841, 822, 800, 782, 754, 727, 698, 538. Mass spectrum (*m/e*): 328 (M^+), 224, 223, 104. Anal. Calcd for $C_{18}H_{18}Nb$: C, 65.86; H, 5.83. Found: C, 65.28; H, 5.85.

$Cp_2Nb(CH_2{=}CHC_6H_4\text{-}p\text{-}CF_3)H$ (8). The above procedure (for **7**) was followed with **6** (0.8 g, 3.54 mmol) and 1.5 mL (9 mmol) of *p*-(trifluoromethyl)styrene. Precipitation yielded 850 mg (61%) of yellow-green microcrystalline **8**. IR (Nujol): 1720, 1601, 1508, 1320, 1219, 1180, 1148, 1103, 1060, 1005, 839, 809, 779, 714. Mass spectrum (*m/e*): 396 (M^+), 243, 242, 224, 223, 172, 159. Anal. Calcd for $C_{19}H_{18}F_3Nb$: C, 57.59; H, 4.58. Found: C, 56.99; H, 4.55.

$Cp_2Nb(CH_2{=}CHC_6H_4\text{-}p\text{-}OMe)H$ (9). The above procedure (for **7**) was followed with **6** (124 mg, 0.55 mmol) and 0.25 mL (1.9 mmol) of *p*-methoxystyrene. Precipitation yielded 146 mg (74%) of yellow-green microcrystalline **9**. IR (Nujol): 3085, 3068, 3018, 1740, 1713, 1695, 1600, 1567, 1502, 1440, 1299, 1289, 1242, 1229, 1160, 1148, 1140, 1101, 1060, 1032, 1016, 1009, 836, 793, 779, 720. Mass spectrum (*m/e*): 358 (M^+), 224, 223, 134. Anal. Calcd for $C_{19}H_{21}ONb$: C, 63.70; H, 5.91. Found: C, 63.28; H, 5.81.

$Cp_2Nb(CH_2{=}CHC_6H_4\text{-}p\text{-}NMe_2)H$ (10). The above procedure (for **7**) was followed with **6** (0.740 g, 3.27 mmol) and 1.3 mL (8.5 mmol) of *p*-(dimethylamino)styrene. Precipitation yielded 1.1 g (91%) of yellow-microcrystalline **10**. IR (Nujol): 3077, 3029, 1717, 1610, 1552, 1512, 1341, 1299, 1234, 1218, 1190, 1163, 1148, 1111, 1058, 1013, 1006, 945, 849, 838, 807, 780, 720. Mass spectrum (*m/e*): 371 (M^+), 224, 223, 147. Anal. Calcd for $C_{20}H_{24}NNb$: C, 64.69; H, 6.52; N, 3.77. Found: C, 64.50; H, 6.54; N, 3.82.

$Cp_2Nb(C{\equiv}NMe)(NMe_2)$. Methyl isocyanide (300 Torr in ≈400 mL at 298 K, 6.5 mmol) was condensed into a solution of **6** (512 mg, 2.27 mmol) in 30 mL of petroleum ether at −78 °C. This mixture was allowed to warm to 25 °C and stirred for 48 h resulting in a maroon solution. This solution was filtered, concentrated to about 20 mL, and slowly cooled to −78 °C to afford 592 mg (84% yield) of the pure product as violet needles. IR (Nujol): 3100, 2789, 2715, 1879 (m), 1782 (vs), 1414, 1260, 1218, 1164, 1108, 1014, 996, 955 (s), 943, 794 (s). Mass spectrum (*m/e*): 308 (M^+), 267, 224, 223. Anal. Calcd for $C_{14}H_{19}N_2Nb$: C, 54.56; H, 6.21; N, 9.09. Found: C, 54.54; H, 6.09; N, 9.02.

Competitive Binding Measurements. Samples of the permethylniobocene meta-substituted styrene hydride complexes, benzene-d_6 and a known amount of ethylene, or permethylniobocene ethylene hydride, benzene-d_6, and a known amount of meta-substituted styrene, were sealed in an NMR tube under argon and allowed to come to equilibrium at room temperature. Similarly, niobocene styrene complex (**7**) with excess propene or one of the substituted styrenes or samples of compounds **8–10**, **16** with excess styrene were prepared in benzene-d_6 and sealed under argon in an NMR tube. These were allowed to reach equilibrium at 25 °C, and the equilibrium constants were determined by measuring the amounts of each species by ^1H NMR (500 MHz). Errors were determined by estimation of the integration errors and by comparing the values obtained by approaching the equilibrium from different sides.

Difference NOE Experiments. All difference NOE experiments were carried out on the WM-500 spectrometer. In the experiment to assign the isomers, each of the four Cp resonances was selectively irradiated and the resulting spectrum subtracted from the standard spectrum, allowing the complete correlation of the various vinylic and hydride signals with the proper Cp signal. A second experiment was performed at −10 °C in toluene-d_8 in which each of the eight hydride and vinylic resonances was selectively irradiated in order to determine the extent of the NOE enhancement between the exchanging sites. The results showed no observable NOE enhancement between the exchanging hydride and vinylic signals although some was observed between the cyclopentadienyl and vinylic signals.

(24) Baldwin, J. E.; Kapecki, J. A. *J. Am. Chem. Soc.* **1970**, *92*, 4869–4873.

(25) Bell, R. A.; Cohen, S. A.; Doherty, N. M.; Threlkel, R. S.; Bercaw, J. E. *Organometallics* **1986**, *5*, 972–975.

(26) (a) Green, M. L. H.; Moreau, J. J. E. *J. Organomet. Chem.* **1978**, *161*, C25–C26. (b) Bunker, M. J.; De Cian, A.; Green, M. L. H.; Moreau, J. J. E.; Siganporia, N. *J. Chem. Soc., Trans.* Dalton **1980**, *2155*–2161. (c) Green, M. L. H.; Jousseaume, B. *J. Organomet. Chem.* **1980**, *193*, 339–344. (d) Curtis, M. D.; Bell, L. G.; Butler, W. M. *Organometallics* **1985**, *4*, 701–707.

(27) Labinger, J. A.; Wong, K. S. *J. Organomet. Chem.* **1979**, *170*, 373–384.

Table X. Summary of Crystal Data for $Cp^*_2Nb(CH_2CHC_6H_5)H$ (2)

formula = $C_{28}H_{39}Nb$
space group *Pbca*
formula wt = 468.5
T = 21 °C
V = 4813 (1) Å^3
z = 8
a = 14.626 (3) Å
b = 18.134 (4) Å
c = 18.147 (4) Å
λ(Mo Kα) = 0.71073 Å
scan range 1.0° above $K\alpha_1$, 1.0° below $K\alpha_2$
reflections $+h$, $+k$, $\pm l$
collected 8188 reflections
averaged 4124 reflections ($3742I > 0$, $2644I > 3\sigma_I$)

Measurement of Olefin Insertion Rates with Coalescence Techniques. Coalescence temperatures of the two C_5R_5 resonances for the olefin hydride complexes **3–5**, **13**, **14** were measured at 90 MHz on a JEOL FX90Q spectrometer. A typical sample was prepared in a glovebox by loading the olefin hydride complex (≈20 mg) and benzene-d_6 (0.4 mL) in a sealable NMR tube. Tubes were sealed either at −196 °C under an atmosphere of nitrogen or at −78 °C under 700 Torr of argon. The temperature at which coalescence occurs was measured by the peak separation of an ethylene glycol sample. The room temperature ^1H NMR spectrum was recorded before and after determination of the coalescence temperature; no decomposition was evident. The rate of exchange at the coalescence temperature was calculated with the Gutowsky–Holm approximation, $k_{exchange}(T_c) = (\pi/\sqrt{2})\Delta\nu$,[28] where $\Delta\nu$ is the frequency separation between the C_5R_5 peaks in the room temperature spectrum. The rate of insertion in these cases is related to the exchange rate by a factor of 2: $k_1(T_c) = 2k_{exchange}(T_c) = \sqrt{2}\pi\Delta\nu$. $\Delta G^\ddagger(T_c)$ can be calculated from the Eyring equation, $\Delta G(T_c) = RT_c \ln (\kappa kT_c/k_c h)$,[29] assuming a transmission coefficient, κ, of 1.

Measurement of Olefin Insertion Rates with Magnetization Transfer Techniques. All magnetization transfer experiments were performed on a Bruker WM-500 spectrometer. Samples were prepared as described above for the coalescence experiments. The sample temperature was maintained by the WM-500 variable-temperature unit and was determined to be constant to within ±1 °C by measuring the temperature before and after the experiment with an ethylene glycol sample. For some of the higher temperature experiments (≥80 °C) the appearance of the sample and the NMR spectrum indicated a small amount of decomposition (≤3%), but this did not appear to affect the results. The relaxation times (T_1) were measured at each temperature by an inversion recovery pulse sequence and analyzed by a three-parameter fitting routine. Magnetization transfer experiments were performed by selectively inverting one of the exchanging signals with a single decoupler pulse and then waiting a variable delay time (τ) before executing the observation pulse. Measurements were generally made for 15–20 τ values spanning a range from milliseconds to several times the T_1 values. The spectrometer's automatic integration routine was used to obtain lists of the peak areas. Peak intensities were determined as ratios of the areas of the exchanging resonances to a constant resonance. A four-parameter nonlinear least-squares fit of the differences of the inverted resonance and the exchanging resonance as a function of delay time to the magnetization equation was performed with a version of the computer program written by Perkin.[30] Errors in k_1 were propagated from the standard deviation calculated for $k_{exchange}$ by the curve-fitting routine.

Structure Determination of $Cp^*_2Nb(CH_2{=}CHC_6H_5)H$ (2). Data Collection. A yellow crystal of $Cp^*_2Nb(CH_2{=}CHC_6H_5)H$ (**2**), grown from petroleum ether/benzene (1:1), was mounted in a glass capillary under a nitrogen atmosphere. A series of oscillation and Weissenberg photographs established the crystal as orthorhombic. Unit cell parameters were obtained by least-squares refinement of fifteen centered reflections (22° < 2θ < 33°): a = 14.626 (3) Å, b = 18.134 (4) Å, c = 18.147 (4) Å, α, β, γ = 90°. The systematic absences led to the unambiguous assignment of the space group P_{bca} ($h0l$: l = odd; $0kl$: k = odd; $hk0$: h = odd).

A total of 8188 reflections (+h, +k, ±l, 4° < 2θ < 30°) were collected on a locally modified Syntex $P2_1$ diffractometer with graphite monochromator and Mo radiation (λ = 0.7107 Å). Three check reflections were remeasured after every 197 reflections, and no decay was indicated. No absorption corrections were applied (μ = 0.49 mm^{-1}, 0.25 < μd < 0.38). A summary of the data collection information is given in Table X.

Structure Determination and Refinement. The coordinates of the niobium atom were derived from the Patterson map; subsequent Fourier and difference Fourier maps revealed the remainder of the structure. Several cycles of full-matrix least-squares refinement with anisotropic

(28) Sandstrom, J. *Dynamic NMR Spectroscopy*; Academic: London, England, 1982; Chapter 6.
(29) Reference 28, Chapter 7.
(30) Perkin, T. Ph.D. Thesis, California Institute of Technology, 1981.

Table XI. Final Parameters[a]

	x	y	z	U_{eq}[b]
Nb	7052 (2)	18814 (2)	14413 (2)	273 (1)
C1	19543 (28)	18792 (27)	22017 (22)	402 (10)
C2	11662 (31)	17498 (22)	26510 (21)	369 (10)
C3	10431 (33)	10979 (24)	31346 (22)	442 (11)
C4	1929 (37)	8076 (26)	32966 (24)	526 (13)
C5	1038 (42)	1945 (29)	37493 (27)	633 (15)
C6	8663 (50)	−1297 (29)	40601 (30)	773 (17)
C7	17031 (46)	1667 (33)	39233 (32)	775 (17)
C8	17985 (37)	7735 (28)	34674 (27)	608 (13)
ring carbons[c]				
C11	10378 (30)	31508 (24)	10348 (24)	425 (10)
C12	8717 (30)	32129 (21)	19327 (21)	356 (10)
C13	−448 (29)	29903 (21)	19327 (21)	356 (10)
C14	−4503 (28)	28141 (23)	12553 (21)	386 (10)
C15	1978 (31)	29274 (21)	6950 (22)	378 (10)
C11M	19006 (37)	33826 (27)	6547 (28)	629 (14)
C12M	14952 (35)	35671 (23)	23447 (28)	562 (13)
C13M	−5419 (32)	30523 (25)	26632 (23)	537 (12)
C14M	−14579 (33)	26742 (29)	11456 (27)	591 (14)
C15M	−195 (39)	30012 (25)	−1135 (24)	582 (13)
C21	16817 (30)	10159 (24)	7787 (24)	408 (11)
C22	10412 (30)	12891 (23)	2611 (22)	377 (10)
C23	1556 (30)	10431 (23)	4861 (23)	379 (10)
C24	2726 (32)	6034 (23)	11265 (24)	414 (11)
C25	12109 (33)	5813 (22)	12982 (23)	413 (11)
C21M	27030 (34)	10670 (34)	6813 (30)	714 (17)
C22M	12953 (35)	16230 (26)	−4633 (23)	508 (12)
C23M	−7236 (37)	10820 (27)	628 (25)	583 (12)
C24M	−4486 (36)	1420 (26)	14894 (29)	621 (13)
C25M	16576 (41)	474 (26)	18273 (27)	641 (15)

[a] $x, y, z \times 10^5$; $U_{eq} \times 10^4$. [b] $U_{eq} = 1/3\sum_i\sum_j U_{ij}(a_i^*a_j^*)a_i^*\cdot a_j^*$; $\sigma U_{eq} = 6^{-1/2}\langle\sigma U_{ii}/U_{ii}\rangle U_{eq}$. [c] Ring methyls denoted by M. C11–C15 correspond to R1 and C21–C25 correspond to R2 (see Figure 6).

Table XII. Distances and Angles

atom	atom	dist (Å)	atom	atom	dist (Å)
Nb	C1	2.289 (4)	C1	C2	1.431 (6)
	C2	2.309 (4)		H1A	1.002 (40)
	C11	2.466 (4)		H1B	1.022 (38)
	C12	2.506 (6)	C2	C3	1.483 (6)
	C13	2.458 (4)		H2	0.930 (41)
	C14	2.415 (4)	C3	C4	1.382 (7)
	C15	2.446 (4)		C8	1.390 (7)
	C21	2.439 (4)	C4	C5	1.389 (7)
	C22	2.446 (4)	C5	C6	1.381 (8)
	C23	2.442 (4)	C6	C7	1.359 (9)
	C24	2.469 (4)	C7	C8	1.384 (8)
	C25	2.484 (4)			
	H	1.752 (33)			
	R1[a]	2.143			
	R2[a]	2.140			

atom	atom	atom	angle (deg)
C1	C2	C3	124.4 (4)
C2	C3	C4	122.6 (4)
C3	C4	C5	121.0 (5)
C4	C5	C6	120.4 (5)
C5	C6	C7	119.0 (6)
C6	C7	C8	121.0 (6)
C2	C3	C8	119.9 (4)
C3	C8	C7	121.1 (5)
C3	C4	C8	117.5 (4)
C1	Nb	C2	36.3 (1)
C1	Nb	H	106.2 (11)
C2	Nb	H	70.5 (11)
R1[a]	Nb	R2[a]	141.4

[a] R1 and R2 are the centroid coordinates of the Cp* rings (see Figure 6).

Gaussian amplitudes for all non-hydrogen atoms resulted in $R = \{\sum W|F_o| - |F_c/k|W/|F_o|\} = 0.0588$ (3264 reflections with $I > 0$) and GOF = $\{\sum W(F_o^2 - F_c^2/k)^2/(n_o - n_p)\}^{1/2} = 1.51$, where n_o is the number of reflections and n_p is the number of parameters (4124 reflections). The parameters for the Cp* hydrogens H111-H253 and the phenyl ring H4-H8 were not refined. There was no residual electron density greater than 0.4 $e^-/Å^3$ remaining in the final difference Fourier map. The final values for the atom coordinates are given in Tables XI and XII; bond lengths and angles are located in Table XII.

The molecular structure of $Cp^*_2Nb(CH_2{=}CHC_6H_5)H$ is shown in Figure 5; a skeletal view of niobium coordination with notable bond lengths and angles is shown in Figure 6.

Acknowledgment. This work was supported by the USDOE Office of Energy Research, Office of Basic Energy Sciences (Grant No. DE-FG03-85ER13431), by the National Science Foundation (Grant CHE-8303735), and by the Shell Companies Foundation, which are gratefully acknowledged. The use of the Southern California Regional NMR Facility, supported by the National Science Foundation Grant No. CHE-84-40137, is also gratefully acknowledged.

Registry No. 1, 93558-77-1; **2**, 95313-63-6; **3**, 113628-22-1; **4**, 113628-23-2; **5**, 113628-24-3; **6**, 11105-67-2; *endo*-**7**, 113628-25-4; *exo*-**7**, 113667-63-3; *endo*-**8**, 113628-26-5; *exo*-**8**, 113667-64-4; *endo*-**9**, 113628-27-6; *exo*-**9**, 113667-65-5; *endo*-**10**, 113628-28-7; *exo*-**10**, 113667-66-6; **11**, 11105-70-7; **12**, 95313-60-3; **13**, 66786-38-7; **14**, 100701-96-0; *endo*-**15**, 95313-62-5; *endo*-**16**, 75576-71-5; *exo*-**16**, 75599-42-7; *endo*-**17**, 113667-67-7; *endo*-**18**, 68586-68-5; *exo*-**18**, 68680-01-3; $Cp_2Nb(C{\equiv}NMe)(NMe_2)$, 113628-29-8; *m*-(trifluoromethyl)styrene, 402-24-4; *m*-methylstyrene, 100-80-1; *m*-(dimethylamino)styrene, 5339-11-7; styrene, 100-42-5; *p*-(trifluoromethyl)styrene, 402-50-6; *p*-methoxystyrene, 637-69-4; *p*-(dimethylamino)styrene, 2039-80-7; methyl isocyanide, 593-75-9.

Supplementary Material Available: Hammett plots for $Cp_2Nb(CH_2{=}CHC_6H_4\text{-}p\text{-}X)H$ insertion rates versus σ_+ and transition-state energies versus σ_p and σ_+, the corrected and uncorrected Eyring plots for *endo*-$Cp^*_2Nb(CH_2{=}CHC_6H_5)H$, and tables of hydrogen idealized positional parameters and thermal parameters and Gaussian amplitudes for all non-hydrogen atoms (6 pages); a listing of structure factors (17 pages). Ordering information is given on any current masthead page.

Heterogeneous, Platinum-Catalyzed Hydrogenation of (Diolefin)dialkylplatinum(II) Complexes: Kinetics[1]

Timothy M. Miller, Alan N. Izumi, Yen-Shiang Shih, and George M. Whitesides*

Contribution from the Department of Chemistry, Harvard University, Cambridge, Massachusetts 02138. *Received July 2, 1987*

Abstract: (Diolefin)dialkylplatinum(II) complexes $[(Ol_2)PtR_2]$ are rapidly reduced by dihydrogen in the presence of platinum black catalyst: the organic groups are converted to alkanes, and the platinum(II) to platinum(0). This platinum(0) is incorporated into the surface of the platinum black catalyst. The reaction is a heterogeneous process catalyzed by platinum(0). Its rate is strongly influenced by mass transport and by the surface area of the catalyst. It is poisoned by dineopentylmercury, di-*n*-octyl sulfide, and tri-*tert*-butylphosphine. Because the catalyst surface is constantly renewed by deposition of platinum, the reaction is, however, less sensitive to poisoning than more familar platinum-catalyzed reactions such as hydrogenation of olefins. The form of the kinetic rate law observed for reduction of (1,5-cyclooctadiene)dimethylplatinum(II) (**1**) depends on the reaction conditions. Two limiting kinetic regimes are observed. In one, mass transport of dihydrogen to the catalyst surface is rate-limiting; in the second, a reaction occurring on the platinum surface is rate-limiting. The activation energy for reaction in the mass transport limited regime is ~3 kcal/mol and that in the reaction rate limited regime is ~15 kcal/mol. In neither regime is there a kinetic isotope effect: $v_{H_2}/v_{D_2} \approx 1.0$. Examination of the relative rates of reaction of a series of (diolefin)dialkylplatinum(II) complexes indicates that the structure of the diolefin has a greater influence on the rate of reaction than does that of the alkyl group. Competitive experiments show that rates are influenced by adsorption of the $(Ol_2)PtR_2$ complex to the catalyst. These studies suggest that the platinum-catalyzed reaction of $(Ol_2)PtR_2$ with dihydrogen takes place by a mechanism analogous to that of the platinum-catalyzed heterogeneous hydrogenation of olefins: the $(Ol_2)PtR_2$ complex chemisorbs on the surface of the platinum catalyst; its organic groups are converted to platinum surface alkyls; coupling of these surface alkyls with surface hydrogen atoms generates the alkane products. The platinum atom originally present in the soluble complex is incorporated into the surface of the platinum catalyst and becomes the reactive site for a subsequent cycle of chemisorption and reaction. The reaction of $(Ol_2)PtR_2$ complexes with dihydrogen thus provides a new method for generating platinum-surface alkyls under conditions representative of those used in heterogeneous platinum-catalyzed processes.

This and the accompanying papers[2,3] describe studies of the reaction of (diolefin)dialkylplatinum(II) complexes $[(Ol_2)PtR_2]$ with dihydrogen in the presence of a platinum black catalyst (eq 1). We demonstrate that this process is a heterogeneous platinum-catalyzed reduction of the soluble organoplatinum compound.

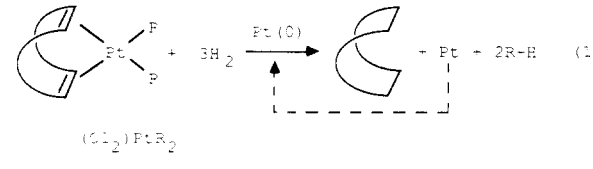

It involves steps broadly analogous to those taking place in platinum-catalyzed heterogeneous hydrogenation of olefins: chemisorption of the organoplatinum compound and dihydrogen

(1) This research was supported by National Science Foundation Grant CHE 85-08702.
(2) Miller, T. M.; McCarthy, T. J.; Whitesides, G. M. *J. Am. Chem. Soc.*, following paper in this issue.
(3) Miller, T. M.; Whitesides, G. M. *J. Am. Chem. Soc.*, second following paper in this issue.

0002-7863/88/1510-3146$01.50/0 © 1988 American Chemical Society